# **Prototypical Contrastive Language Image Pretraining**

Delong Chen<sup>1,2</sup>, Zhao Wu<sup>1</sup>, Fan Liu<sup>2</sup>, Zaiquan Yang<sup>1,3</sup>, Yixiang Huang<sup>1,4</sup>, Yiping Bao<sup>1</sup>, and Erjin Zhou<sup>1</sup>

<sup>1</sup>MEGVII Technology <sup>2</sup>Hohai University <sup>3</sup>Beijing University of Aeronautics and Astronautics <sup>4</sup>Beijing University of Posts and Telecommunications

## **Abstract**

Contrastive Language Image Pretraining (CLIP) received widespread attention since its learned representations can be transferred well to various downstream tasks. During CLIP training, the InfoNCE objective aims to align positive imagetext pairs and separate negative ones. In this paper, we show a representation grouping effect during this process: the InfoNCE objective indirectly groups semantically similar representations together via randomly emerged within-modal anchors. We introduce Prototypical Contrastive Language Image Pretraining (ProtoCLIP) to enhance such grouping by boosting its efficiency and increasing its robustness against modality gap. Specifically, ProtoCLIP sets up prototype-level discrimination between image and text spaces, which efficiently transfers higherlevel structural knowledge. We further propose Prototypical Back Translation (PBT) to decouple representation grouping from representation alignment, resulting in effective learning of meaningful representations under large modality gap. PBT also enables us to introduce additional external teachers with richer prior knowledge. ProtoCLIP is trained with an online episodic training strategy, which makes it can be scaled up to unlimited amounts of data. We train our ProtoCLIP on Conceptual Captions and achieved an +5.81% ImageNet linear probing improvement and an +2.01% ImageNet zero-shot classification improvement. On larger YFCC dataset, ProtoCLIP matches the performance of CLIP with 4×fewer pretraining epochs. Codes are available at https://github.com/megvii-research/protoclip.

# 1 Introduction

Contrastive Language Image Pretraining (CLIP) [1, 2] has achieved impressive performance on learning representations from large-scale image-text pairs collected from the Internet. It optimizes the InfoNCE objective [3] during pretraining, but how this simple objective derives meaningful image-text representations is not well studied. Intuitively, the InfoNCE objective creates a joint representation space, where paired image-text representations are pushed together and unpaired representations are pulled apart. This property can be termed as *representation alignment*. However, fulfilling this alone is inadequate for perfect downstream performance. For example, the image-text representations can be perfectly aligned [4] and randomly distributed at the same time. In such a situation, the InfoNCE objective can still reach its minimum but the downstream performance would be poor [5].

This contradiction motivated us to seek a new understanding of CLIP's learning process beyond representation alignment. We find the recent "augmentation overlap" [5] theory is particularly instructive for this. As shown in Figure 1(a), in contrastive visual pretraining (e.g., SimCLR [6]), aggressive image augmentations are randomly applied to generate different views. The "augmentation

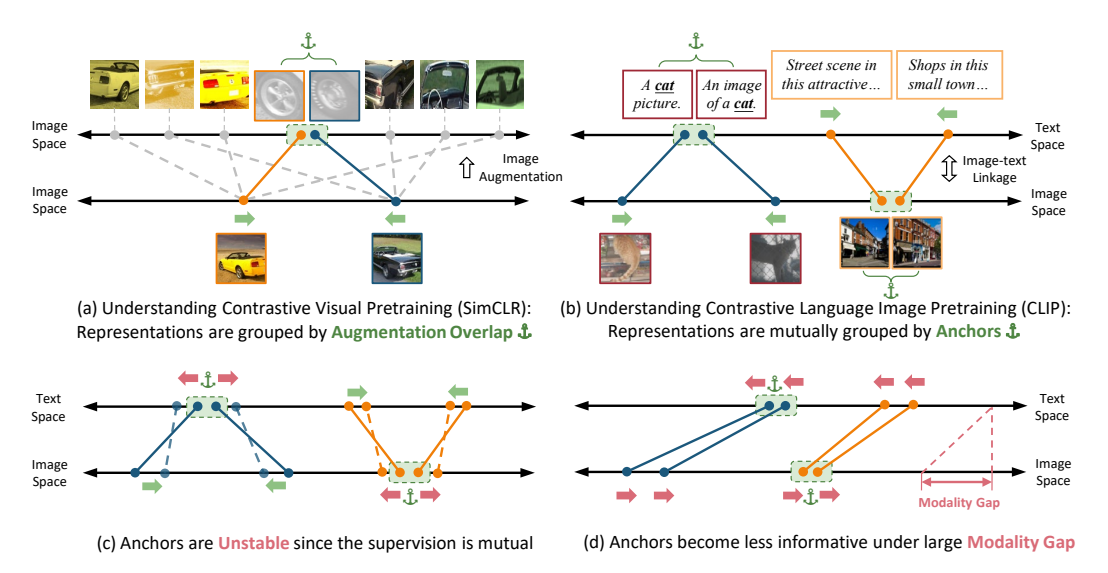


Figure 1: Illustrations of representation grouping in 1-dimensional spaces. Each "•—•" represents an image-image (a) or image-text representation (b)-(d) pair.

overlap" [5] theory suggests that pairs of indistinguishable views (e.g., the wheels of two different cars, noted by the green dashed box) will emerge during this process. When the InfoNCE objective aligns different views together, these overlapped augmentations will group intra-class samples together (as noted by green arrows). By regarding different modalities as different views, we can naturally extend the above theory to a multimodal setting. As in Figure 1(b), now the inherent linkage of image-text pairs plays a similar role to image augmentations. Close within-modality pairs (noted by green dashed boxes) will emerge and serve as "anchors" to group the corresponding representations in the opposite modality. For example, robust visual features (e.g., recognizing cats from different angles) can be learned through the co-occurrence of the word "cat" in a pair of text captions.

Such representation grouping of InfoNCE has been demonstrated to be effective, but our new "anchorgrouping" understanding reveals its two major weaknesses. First, the grouping is done in an indirect manner, anchors are prone to be pulled apart by the "reaction" from the immature opposite modality. When the text anchor in Figure 1(b) pushes two cat images together (i.e., learning robust visual representations as desired, as green arrows in Figure 1(c)), the large distance between these immature image representations would separate the text anchor apart (for example, learning to discriminate word "picture" and "image" undesirably, as red arrows in Figure 1(c)). Such "reaction" leads to a reduced number of effective anchors and yields less grouped representations. **Second**, anchors become less informative with the existence of a large modality gap. Modality gap [7] is defined as the range between mean representations in image and text spaces. As shown in Figure 1(d), when the two representation spaces are not overall aligned, the InfoNCE objective will focus primarily on aligning them to minimize the modality gap rather than learning meaningful representations via anchorgrouping since the large gap overwhelms the relational information within each modalities. A similar problem has been well explored in the field of knowledge distillation [8], where researchers found that the "absolute teacher" is not robust to representation space translation—a single modal version of modality gap—and yields sub-optimal performance [9]. Unfortunately, at the beginning of CLIP training, a large modality gap occurs with a very high possibility due to the independent initialization of CLIP's two encoders and the inherent "cone effect" of non-linear deep neural networks [7].

We propose **Proto**typical **C**ontrastive **L**anguage **I**mage **P**retraining (ProtoCLIP) to solve these issues. We construct and dynamically update prototypes on both image and text spaces and use them to *directly* supervise the opposite modality. This leads to richer supervision signals and more efficient representation grouping: prototypes are more stable than randomly emerged anchors since they are fixed targets for the opposite side and thus are not at the risk of being pulled apart. For modality gap, we further introduce a simple yet effective **P**rototype **B**ack **T**ranslation (PBT) technique to decouple representation grouping from representation alignment. PBT calculates a within-modal centroid for samples that are assigned to a shared prototype, and then groups these representations towards the centroid. With PBT, representation alignment is no longer a prerequisite for effective learning of

representation grouping. Based on the ability to learn representations from unaligned spaces, we can further introduce an external teacher (e.g., a pretrained RoBERTa [10]) with richer prior knowledge.

Furthermore, we present two improvements to previous clustering-based pretraining methods. **First**, many previous methods [11–17] update the clusters after each training epoch or several consecutive epochs. Such a training strategy can work well on medium-sized ImageNet [18] but is not scalable to larger datasets (e.g., YFCC [19]) due to low cluster updating frequency. To train the ProtoCLIP more efficiently, we design an online episodic training strategy, which makes the training of ProtoCLIP can be scaled up to unlimited amounts of data. **Second**, previous works [11, 13–16, 20] learn one-hot pseudo labels as hard targets, which ignores the structural relationship among clusters. To this end, we convert hard cluster assignment to probability scores by softmax to enable the effective transfer of such relational knowledge. Overall, our main contributions in this paper are summarized as the following:

- We proposed ProtoCLIP with prototype-level discrimination that enables more efficient representation grouping in large-scale vision-language pretraining. Prototypes serve as stable anchors to group the representations of semantically similar samples together.
- We designed PBT to translate cross-modal prototypes to within-modal centroids. PBT enables ProtoCLIP to learn meaningful representations between unaligned spaces. Via PBT, we further introduced pretrained RoBERTa as an external teacher for richer supervision.
- We presented two improvements to previous clustering-based pretraining methods: 1)
   online episodic training strategy that improves cluster updating frequency, and 2) the use of
   probability-based soft targets which transfer structural relational knowledge.
- Experimental results on Conceptual Captions showed that ProtoCLIP outperforms CLIP by +5.81% and +2.01% on ImagNet linear probing and zero-shot classification respectively. On larger YFCC dataset, ProtoCLIP matched the performance of CLIP with 4×fewer epochs.

# 2 Related Works

Vision Language Pretraining. Recent works have exploited learning multimodal representations from large-scale uncurated web-crawled image-text data and showed promising results. 1) Singlestream models [21-24] fuse image and text based on the advantage of the self-attention mechanism [25] and excel at multimodal fusing and understanding, leading to impressive performance on high-level multimodal tasks such as Visual Question Answering (VQA) and image captioning. Unfortunately, the transferability of single-stream models is weak since they have no independent encoder that can be transferred to single modal tasks. 2) Dual-stream models set up two separated encoders to align visual and textual representations. Though the methodology is quite simple, pioneer works [1, 2]) demonstrated prestigious success when combining it with a huge amount of training data. Some follow-up works improved CLIP from the representation alignment perspective. For example, FILIP [26] introduced finer-grained representation alignment to boost multimodal interaction. CLOOB [27] introduced Hopfield Networks for improved learning of feature associations and co-occurrences. More recent efforts focus on improving the learning efficiency, since the training of CLIP is highly expensive. To improve the learning efficiency, EfficientCLIP [28] and SLIP [29] respectively combined BERT [30]-style and SimCLR [6]-style single-modal self supervision with CLIP. DeCLIP [31] further integrates multi-view supervision and nearest-neighbor supervision.

Self-supervised Visual Representation Learning. Self-supervised Learning (SSL) [32] aims at learning meaningful representations without human supervision. Early works on SSL focus on exploring pretext tasks [33]. After SimCLR [6] demonstrated the effectiveness of instance discrimination task, contrastive learning became dominant. SimCLR aligns representations of different data augmentations, which creates augmentation overlaps [5] that groups intra-class samples together. Unfortunately, SimCLR relies on extremely large batch sizes for sufficient negatives. To solve this issue, MoCo [34] introduced momentum contrast, while BYOL [35] and SimSiam [36] showed that representations can be learned without negatives. Though these works effectively improved SSL learned representations, they share a fundamental weakness that the model is only encouraged to learn augmentation-invariant representations, while higher levels of semantic relations are ignored. Nearest Neighbor-based methods such as NNCLR [37] and MYOL [38] introduced richer supervision signals, but the variance of positive pairs is still limited.

Clustering-based SSL. A promising line of work in SSL is clustering-based approaches. Deep-Cluster [11] and SeLa [13] assign pseudo labels using *K*-Means or Sinkhorn Knopp algorithm, then use these labels to supervise model training. SwAv [12] contrasts the cluster assignment between different augmentations of the same image. The clustering of SwAV is done in an online fashion, but it forces the size of each cluster to be equal. PCL [14] and SCCL [20] combined cluster-level contrast with instance-level contrast and demonstrated the effectiveness in image SSL and text SSL respectively. XDC [15] and SeLaVi [16] respectively extend DeepCluster [11] and SeLa to audiovisual pretraining [13]. ProtoCLIP shares some similarities with XDC [15], since both of them utilize the clusters in the opposite modality as supervision. However, ProtoCLIP aims at VLP instead of audiovisual pretraining which only requires representation grouping—in a VLP scenario, representation alignment should be considered as well for zero-shot classification and cross-modal retrieval. Besides, compared to a pure VLP version of XDC, ProtoCLIP contains several novel designs, including PBT, episodic training, learnable temperature, and the use of soft targets.

# 3 Method

## 3.1 Prototypical Contrastive Language Image Pretraining

Let's get started by revisiting the InfoNCE objective used by the original CLIP [1]. CLIP is trained with large-scale image-text dataset  $\mathcal{D} = \{(x_i^I, x_i^T)\}_{i=1}^M$  that consists of a total of M training samples. The goal is to learn an image encoder  $f^I$  and a text encoder  $f^T$  that respectively encode  $x_i^I$  and  $x_i^T$  to their latent representations, i.e.,  $f^I(x_i^I) = z_i^I \in \mathbb{R}^{d_z \times 1}$  and  $f^T(x_i^T) = z_i^T \in \mathbb{R}^{d_z \times 1}$ . The learned representation should fulfill two requirements: representation alignment and representation grouping:

**Representation alignment** refers to high similarity  $z_i^I \cdot z_i^T$  of paired image and text samples  $x_i^I, x_i^T$ , and low similarity  $z_i^I \cdot z_j^T (i \neq j)$  between the unpaired samples  $x_i^I, x_j^T$ . Generally, perfect representation alignment yields strong downstream performance on cross-modal retrieval tasks.

**Representation grouping** means that representations of semantically similar samples are grouped together, while those of dissimilar samples should be pulled apart. Perfect representation grouping yields strong linear classification performance.

While fulfilling perfect representation alignment and representation grouping at the same time, coupled with a large dataset that contains sufficient open-set concepts, the model can achieve strong zero-shot classification performance. To achieve this objective, CLIP creates an instance discrimination task within each batch, and optimizes the following bi-directional InfoNCE objective [3]:

$$\mathcal{L}_{\text{CLIP}} = -\left(\underbrace{\frac{1}{N} \sum_{i=1}^{N} \log \frac{\exp(z_i^I \cdot z_i^T / \tau_{\text{CLIP}})}{\sum_{j=1}^{N} \exp(z_i^I \cdot z_j^T / \tau_{\text{CLIP}})}}_{\text{image to text}} + \underbrace{\frac{1}{N} \sum_{i=1}^{N} \log \frac{\exp(z_i^T \cdot z_i^I / \tau_{\text{CLIP}})}{\sum_{j=1}^{N} \exp(z_i^T \cdot z_j^I / \tau_{\text{CLIP}})}}_{\text{text to image}}\right) / 2, \quad (1)$$

where N is the batch size and  $\tau_{\text{CLIP}}$  is a learnable temperature parameter.

As illustrated in Section 1, representation grouping is done *indirectly* by the InfoNCE objective. Here we want to boost the efficiency by performing representation grouping in a *direct* manner. We raise the instance-level discrimination to prototype-level discrimination by constructing and updating prototypes. A prototype is a representation for a group of semantically similar instances [14]. We push representations the prototype directly for grouping via a proposed prototypical loss  $\mathcal{L}_{Proto}$ .

An illustration of ProtoCLIP architecture is shown in Figure 2. To acquire prototypes, we apply MLP projection heads  $g^I$  and  $g^T$  on top of  $z_i^I$  and  $z_i^T$  respectively, then we get projected representations  $g^I(z_i^I) = h_i^I \in \mathbb{R}^{d_h \times 1}$  and  $g^T(z_i^T) = h_i^T \in \mathbb{R}^{d_h \times 1}$ . We adopt K-Means clustering due to its simplicity and scalability. Other clustering methods can be used here as well. Specifically, we find prototypes  $C^I \in \mathbb{R}^{K \times d_h} = [c_1^I, c_2^I, ..., c_K^I]$  and  $C^T \in \mathbb{R}^{K \times d_h} = [c_1^T, c_2^T, ..., c_K^T]$  that minimize the following K-Means objective:

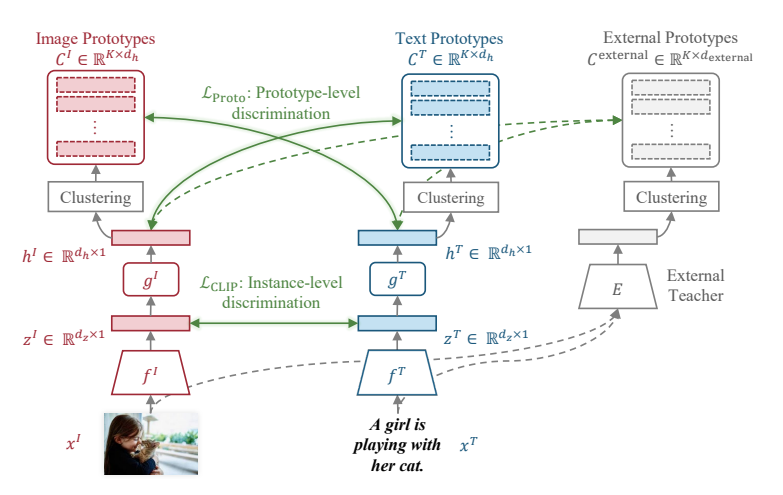


Figure 2: **Model Architecture of ProtoCLIP.** We setup prototype-level discrimination upon the instance-level discrimination. We construct prototypes with representations after projection heads  $g^I$ ,  $g^T$ . The prototypes are used to guide the learning of the opposite modality. An external teacher E is introduced for richer supervision, which will be detailed in Section 3.2.

$$\arg\min_{C^I,C^T} \underbrace{\sum_{k=1}^K \sum_{i=1}^M \left\| g^T(z_i^T) - c_k^T \right\|^2}_{\text{clustering text representations}} + \underbrace{\sum_{k=1}^K \sum_{i=1}^M \left\| g^I(z_i^I) - c_k^I \right\|^2}_{\text{clustering image representations}} \tag{2}$$

Note that this process is operated on detached representations, so that the network would not receive any gradient. After K-Means clustering, pseudo labels (or cluster assignment) can be then generated for each sample according to the closeness between its representation and each prototype . Previous clustering-based audiovisual pretraining method XDC [15] have compared different types of supervision and found model learns the best when it is purely supervised by the opposite modality. Inspired by XDC, Here ProtoCLIP creates prototypical supervision in a cross-modal manner: we use the prototypes in the opposite modality to guide representation learning  $^1$ . Besides, previous methods such as DeepCluster [11] and XDC [15] generate class indices and train an additional parametric classifier with cross-entropy loss, as usually done in traditional supervised training. However, since there is no mapping between two consecutive cluster assignments, such a method requires frequent reinitialization of the classifier, which interrupts the training procedure. Instead, we use the prototypes as linear classifiers directly [12, 14]. As in Eq. 3, we calculate classification scores  $S_i^T \in \mathbb{R}^{k \times 1}$  and  $S_i^T \in \mathbb{R}^{k \times 1}$  by applying the prototype classifier to the cross-modal representations, then normalize the scores to possibilities by taking softmax:

$$\begin{aligned} p_i^I &= \operatorname{softmax}(S_i^I/\tau_{\operatorname{Proto}}), & \text{where} \quad S_i^I &= C^T \cdot h_i^I. \\ p_i^T &= \operatorname{softmax}(S_i^T/\tau_{\operatorname{Proto}}), & \text{where} \quad S_i^T &= C^I \cdot h_i^T. \end{aligned} \tag{3}$$

where  $\tau_{\text{Proto}}$  is the temperature hyper-parameter. Instead setting a fixed temperature as in DeepCluster-v2 [12], we set it to a learnable parameter as in  $\mathcal{L}_{\text{CLIP}}$  since it yields improved results. Now, we can get  $\mathcal{L}_{\text{Proto}}$  by applying the cross entropy loss function:

$$\mathcal{L}_{\text{Proto}} = -(\underbrace{\sum_{i=1}^{M} \sum_{k=1}^{K} y_{i,k}^{T} \log(p_{i,k}^{I})}_{\text{image to text}} + \underbrace{\sum_{i=1}^{M} \sum_{k=1}^{K} y_{i,k}^{I} \log(p_{i,k}^{T}))/2}_{\text{text to image}}, \tag{4}$$

<sup>&</sup>lt;sup>1</sup>We empirically found that multi-modal fusion-based supervision (i.e., the CDC [15]) yields significantly degenerated performances for VLP. The density of initial random text representations is much higher than that of image representations, which makes it dominate the pseudo label generation and failed to learn useful knowledge from the image representations.

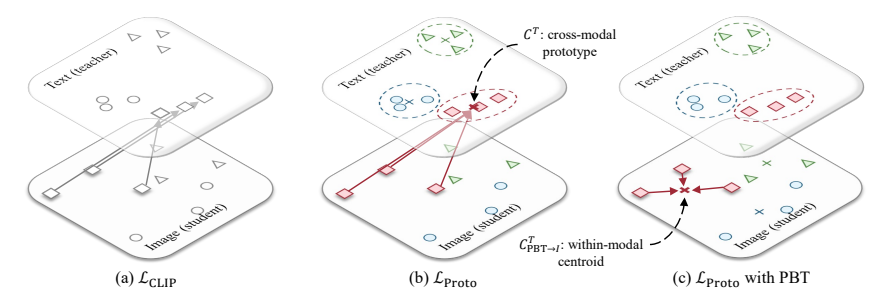


Figure 3: Comparison of  $\mathcal{L}_{\text{CLIP}}$ ,  $\mathcal{L}_{\text{Proto}}$ , and  $\mathcal{L}_{\text{Proto}}$  with PBT. Our PBT translates cross-modal prototypes  $(C^T)$  to within-modal centroids  $(C^T_{\text{PBT} \to I})$  according to prototype assignment. Since both of these losses are bi-directional between image and text spaces, here we only visualize the supervision from text (as teacher) to image (as student).

**Learning from soft targets.** In Eq. 4,  $y_i^T \in \mathbb{R}^{k \times 1}$  and  $y_i^I \in \mathbb{R}^{k \times 1}$  are k-way pseudo target scores. Previous clustering-based methods [11, 13–16] convert class indices to a one-hot vector as target. Such a one-hot target creates a one-vs-all learning task: representations are pushed towards their assigned prototypes *only* and pushed away from other prototypes *equally*. To learn more structured knowledge, we use probability-based soft target to replace the hard one-hot assignment:

$$\begin{aligned} y_k^T &= \operatorname{softmax}(S_k^{\hat{T}}/\tau_{\mathbf{y}}), & \text{where} \quad S_k^{\hat{T}} &= C^T \cdot c_k^T. \\ y_k^I &= \operatorname{softmax}(S_k^{\hat{I}}/\tau_{\mathbf{y}}), & \text{where} \quad S_k^{\hat{I}} &= C^I \cdot c_k^I. \end{aligned} \tag{5}$$

The scores in Eq. 5 are calculated by measuring the dot-product similarity between the "ground truth" prototype  $c_k^I, c_k^T$  and all the prototypes  $C^I, C^T$ . The "ground truth" prototype will have the highest similarity with itself (e.g., "cat" and "cat"), relatively high similarities with its neighboring prototypes (e.g., "cat" and "tiger"), and low similarities with distant prototypes (e.g., "cat" and "car"). When such relational knowledge is embedded in the targets  $y_k^I, y_k^T$ , the ProtoCLIP can learn more structured knowledge. Finally, the ProtoCLIP is trained to minimize  $\mathcal{L}_{\text{Proto}}$  and  $\mathcal{L}_{\text{CLIP}}$  jointly:

$$\mathcal{L}_{ProtoCLIP} = \mathcal{L}_{Proto} + \mathcal{L}_{CLIP}$$
 (6)

# 3.2 Learning Representation Grouping from Unaligned Spaces

We compare the differences between  $\mathcal{L}_{CLIP}$  and  $\mathcal{L}_{Proto}$  in Figure 3(a) and (b). Though  $\mathcal{L}_{Proto}$  improves the representation grouping efficiency, it still suffers from the *modality gap* problem. In Figure 3 (b), all the three data points in the student space would be pushed to the right side in order to align them with the prototype in teacher space.

**Prototype Back Translation.** The core reason of the modality gap problem is that  $\mathcal{L}_{\text{Proto}}$  forces the student representations to be strictly anchored to the position of their prototype in the teacher space. We introduce a simple yet effective technique called Prototype Back Translation (PBT) to avoid this problem. As shown in Figure 3(c), for each prototype in teacher space, we retrieve all the samples that are assigned to it, and then calculate a centroid of the corresponding representations in the student space. We denote the obtained image and text centroids as  $C_{\text{PBT} \to I}^T$  and  $C_{\text{PBT} \to T}^I$  and use them to replace the original prototypes  $C^T$  and  $C^I$  when calculating  $\mathcal{L}_{\text{Proto}}$ . PBT enables knowledge transfer between unaligned representation spaces since student representations are grouped directly to their within-modal centroid instead of pushed towards their cross-modal prototypes. We note that the advantage of  $\mathcal{L}_{\text{Proto}}$  + PBT over plain  $\mathcal{L}_{\text{Proto}}$  are similar to the advantage of Relational Knowledge Distillation (RKD) [9, 39] over traditional Knowledge Distillation (KD) [8]. However, RKD transfers relational knowledge in a per-sample-pair manner, while PBT transfers knowledge via prototypes with a higher level of semantics.

**Learning from External Teacher.** Since representation grouping is decoupled from representation alignment, we can now ensemble multiple teachers to guide the learning of student representations. For example, in addition to the original mutual knowledge transfer between image and text spaces, we can further introduce an external teacher encoder E to distill richer knowledge to ProtoCLIP. As Figure 2, the encoder E can encode either image  $x_i^T$  or text  $x_i^T$ , then external prototypes C external

can be constructed in the resulting representations space by performing K-Means clustering as before. We use PBT to translate the prototypes  $C^{\text{external}}$  to within-modal centroids  $C^{\text{external}}_{\text{PBT} \to T}$  and  $C^{\text{external}}_{\text{PBT} \to T}$ , then an additional loss term  $\mathcal{L}^{\text{external}}_{\text{Proto}}$  can be added by applying the obtained prototype classifier, taking softmax, then calculating cross-entropy loss in a similar way of Eq. 4, and finally  $\mathcal{L}_{\text{ProtoCLIP}} = \mathcal{L}_{\text{Proto}} + \mathcal{L}_{\text{CLIP}} + \mathcal{L}^{\text{external}}_{\text{Proto}}$ .

#### 3.3 Episodic Training

Previous clustering-based methods [11, 13–17] update the clusters after an entire training epoch. Such an approach works well on medium-sized ImageNet [18] dataset since the model can be trained for several hundreds of epochs, resulting in several hundreds of cluster updating. However, CLIP is usually trained for much fewer epochs (e.g., 32 [40]), which makes the frequency of epoch-wise updating insufficient. We propose an *episodic training* strategy. *Episodes* are constructed by randomly choosing  $m \ll M$  samples from the entire dataset. Then, 1) feature extraction, 2) prototype updating, and 3) model training are performed sequentially, and then a new episode is then constructed. Episodic training makes prototype updating frequency independent of dataset size M, enabling ProtoCLIP to be scaled up to unlimited amounts of training data. To benchmark episodic training-based ProtoCLIP with other models that is trained conventionally, the total number of episode  $n_{\rm episode}$  is defined as  $n_{\rm episode} = n_{\rm epoch} \times \frac{M}{m}$ . Episode size m is an important hyper-parameter. Smaller m results in higher prototype updating frequency, but too small m increases the sparsity of representations within an episode. In such situations, samples that are assigned to the same prototypes may have different semantics, which decreases the reliability of prototypes.

# 4 Experiments

## 4.1 Ablation Study of ProtoCLIP Hyper-parameters

This section validates the impact of the hyper-parameters of ProtoCLIP. A one-million subset of the Conceptual Captions (CC) [41] dataset is used. To avoid testset hyper-parameter tuning, CIFAR10, CIFAR100 and STL10 dataset are adopted here for validation. Benchmarks on other downstream datasets will be reported later in Section 4.2 and Section 4.2. Total training amount here (episode size  $\times n_{\rm episode}$ ) is set equivalent to 20 epochs. Following the original setting in CLIP [1], we use the modified ResNet50 [42] and transformer [25] as image and text encoders respectively. The default setting of the ProtoCLIP includes episode size  $m=0.2{\rm M}$ , no soft target, 10 images per prototype, no external teacher, and no data augmentations. K-Means is performed with a max iteration limit of 20 steps, which we found sufficient to converge. More details can be found in the Appendix B.

**Episode Size.** As illustrated in Section 3.3, there exists a trade-off between prototype reliability and updating frequency. Here we try find an optimal episode size that can satisfy both sides by training ProtoCLIP (without  $\mathcal{L}_{\text{CLIP}}$ ) using different episode size. As shown in Figure 4(a), an episode size of 0.2M yields the best performance. The rightmost bar in red (episode size=1M) is equivalent to update the cluster after one entire training epoch as done in previous methods [11, 13–17]. With the best value of episode size, our episodic training strategy leads to a +2.86% improvement.

**Target Temperature.** Next, we turn to select the best target temperature  $\tau_y$ . Though higher value of  $\tau_y$  transfers structural relation knowledge, too large  $\tau_y$  makes target scores to be over-smoothed. Figure 4(b) shows that  $\tau_y$ =0.01 achieves the best performance. Compared to the one-hot label (hardmax, the leftmost bar in red) used in previous clustering-based SSL approaches [11, 13–16, 20], learning from soft target brings +1.58% improvement.

Number of Images per Prototype. Clustering-based SSL for ImageNet pretraining often sets the total number of clusters to be several thousands (e.g., K = 3000 for SwAV [12]). We found that with uncurated image-text dataset, this hyper-parameter should be chosen more conservatively. The reason is that uncurated image-text dataset contains much more concepts than curated ones [43]. Lower K increases the noise within each cluster. We train our model with  $\mathcal{L}_{\text{Proto}} + \mathcal{L}_{\text{CLIP}}$ . Figure 4(c) shows that 10 images per prototype (i.e. K = 20k for an episode size of 0.2M) yield the best performance.

**External Teacher.** Finally, we compare different external teachers. We consider the text encoder of pretrained CLIP (ViT/B-32) [1] and the pretrained RoBERTa [10]. Figure 4(d) shows that both of these two external teacher benefit ProtoCLIP, while RoBERTa brings more improvement.

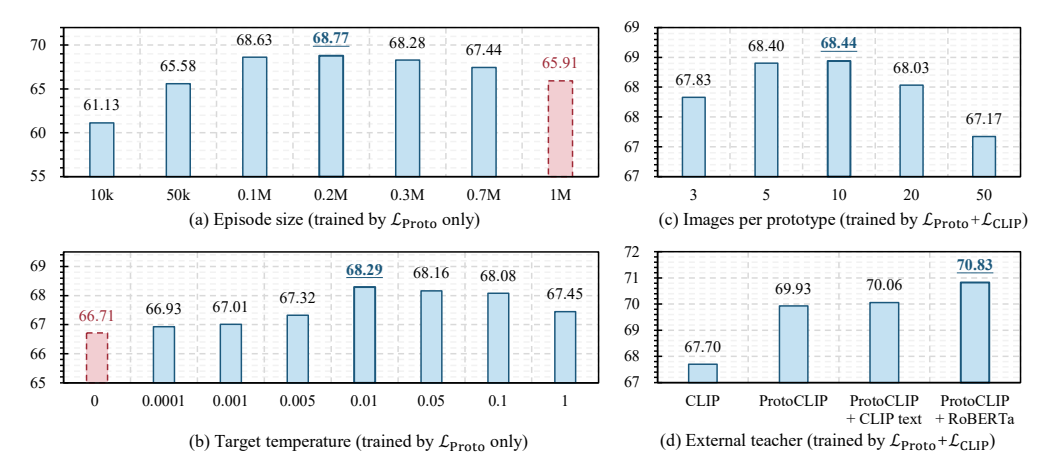


Figure 4: ProtoCLIP ablation experiments on Conceptual Captions 1M data (20 epoch). We report the average linear probing accuracies (%) of CIFAR10, CIFAR100, and STL10. Detailed results are given in Appendix B.

#### 4.2 Conceptual Captions Pretraining

**Pretraining Setting.** With selected hyper-parameters, we now train the ProtoCLIP on full CC data. The original CC dataset [41] (collected in 2018) contains over 3.3M samples. Unfortunately, due to broken links, an increasing number of images become inaccessible. To benefit future benchmarking, we use a total of 2,500,000 samples (CC2.5M) from CC to train our model. We continue to adopt ResNet-50 [42] and transformer [25] as image and text encoders. With a single-node 4×2080Ti machine, training a ProtoCLIP for 32 epochs takes approximately 64 hours. We apply random data augmentations to create implicit contrast.

**Downstream Evaluations.** We perform linear probing and zero-shot classification on ImageNet, CIFAR and STL. We note that CLIP models are usually evaluated on a more diverse downstream datasets. However, since the CC dataset cannot provide sufficient coverage for open-vocabulary visual concepts [43], the downstream performance on these diverse datasets is extremely low (e.g., <10%) and the performance differences between different methods are marginal, making it hard to draw safe conclusion based on the metrics. Instead, we leave comprehensive evaluations on diverse datasets to Section 4.2 when the models are trained with larger YFCC dataset. Moreover, mean recall of MS-COCO [44] cross-modal retrieval is also reported to evaluate representation alignment. More details of experimental setting are presented in the Appendix A.1.

Effectiveness of Each Component. We first validate the effectiveness of each ProtoCLIP component on CC2.5M. We train ProtoCLIP on CC2.5M for 8 epochs, and compare its zero-shot classification and linear probing performance with CLIP and ablations of ProtoCLIP. Classification accuracy on ImageNet and averaged accuracy on CIFAR10, CIFAR100, and STL10 are reported. We first remove the external teacher RoBERTa, then respectively ablate 1) PBT, 2) soft target, 3) *K*-Means optimizing, and 4) data augmentation. As in Table 1(a), full ProtoCLIP achieve the best performance overall. Every other comparison yields degenerated performance, showing the effectiveness of each component. For ImageNet linear probing accuracy, introducing PBT brings +1.83% improvement, while introducing an external teacher brings +1.76% improvement. All these ablations of ProtoCLIP outperform CLIP baseline on most metrics.

**Benchmarking ProtoCLIP.** Next, we benchmark ProtoCLIP by training it on CC2.5M for standard 32 epochs, and further half the epochs of ProtoCLIP or double the epochs of CLIP baseline to compare training efficiency. Table 1(b) summarizes main results. With the same 32 training epochs (line 2 vs. 3), ProtoCLIP outperforms CLIP by +5.81% on ImageNet linear probing and +2.01% on ImageNet zero-shot classification. Impressively, ProtoCLIP can outperform CLIP with 2× fewer training epochs (line 1 vs. 2, line 3 vs. 4), and match the performance of CLIP with even 4× fewer epochs (line 1 vs. 4). At the same time, ProtoCLIP maintains comparable but slightly degenerated (-0.79%) cross-modal retrieval performances. Appendix C presents full results.

Table 1: Conceptual Captions pretraining results. (a): ProtoCLIP ablation experiment on Conceptual Captions 2.5M data (8 epoch). (b): Conceptual Captions pretraining benchmarks. ▷ indicates results reported by corresponding papers.

Method	ImageNet zero-shot	ImageNet linear	CIFAR & STL zero-shot Avg.	CIFAR & STL linear Avg.	Batch Size	Data	Epoch	Method	ImageNet zero-shot top-1	ImageNet zero-shot top-5	ImageNet linear	retrieval mean recall
CLIP	9.89	41.30	38.77	67.32			16	ProtoCLIP	20.39	40.02	50.47	36.01
ProtoCLIP	11.96	46.55	42.74	70.96	512	2.5M	32	CLIP	19.46	38.42	49.41	36.48
ProtoCLIP w/o RoBERTa	11.91	44.76	42.81	69.45	312	2.3111	32	ProtoCLIP	21.47	40.84	55.22	35.69
- w/o PBT	11.23	42.93	42.32	68.89			64	CLIP	20.34	39.21	51.14	37.61
	11.28	44.22	42.66	69.18	512	2.9M	31	▷ CLOOB [27]	23.97	-	-	-
- w/o soft target					312	2.9IVI	31	$\triangleright$ CLIP	20.33	-	-	-
- w/o K-means	11.62	44.27	38.67	67.22	1024	3M	32	DeCLIP [31]	27.2	-	-	-
<ul> <li>w/o augmentation</li> </ul>	11.17	44.39	38.67	68.75	1024	3111	32	$\triangleright$ CLIP	20.6	-	-	-
	(a)							(b)				

Table 2: **YFCC pretraining results.** The performance of ProtoCLIP matched CLIP with 4× fewer pretraining epochs. (a): Performance comparison of zero-shot / linear / K-NN classification and COCO retrieval. "IN": ImageNet, "14/9 Avg.": averaged classification accuracy across datasets. (b):Transfer learning of object detection on MS-COCO with ResNet-50 backbone and Mask-RCNN detector [46].

Arch.	Model	Data	Epcoh	Ze: IN	ro-shot 14 Avg.	Li IN	inear 9 Avg.	IN	-NN 9 Avg.	Retrieval Mean Recall				
RN50	CLIP ProtoCLIP	15M 14M	32 8	32.7 32.0	31.1 31.9	61.5 62.1	65.8 65.4	56.0 56.7	57.8 58.3	40.9 42.7	Method	Epoch	Box AP	Mask AP
				-0.7	+0.8	+0.6	-0.3	+0.8	+0.5	+1.8	CLIP	32	36.5	34.2
RN101	CLIP	15M	32	34.8	32.9	63.1	66.2	57.9	59.0	43.2	ProtoCLIP	8	36.4	34.4
KN101	ProtoCLIP	14M	8	33.8	33.0	62.9	65.4	58.0	59.0	44.7				
				-1.0	+0.1	-0.2	-0.8	+0.2	+0.1	+1.5		(b)		
					(a)									

## 4.3 YFCC Pretraining

**Pretraining Setting.** We train the ProtoCLIP on the YFCC-100M [19] subset YFCC-15M filtered by OpenAI [1], which consists about 15 million of image-text pairs. Due to broken links, we use 14,000,000,000 of them (YFCC-14M) as the pretraining dataset. We used the ResNet-50 [42] as well as larger ResNet-101 backbone. The CLIP checkpoints (YFCC-15M, 32 epochs) released by OpenCLIP [45] are adopted as baseline.

**Downstream Evaluations.** We evaluate pretrained models on the following downstream tasks: 1) Zero-shot Classification. A total of 14 datasets are used, whose descriptions will be given in Appendix B. 2) Linear Probing and 3) K-NN Classification. Linear classifier or K-NN classifier are built with frozen features of the training split. A total of 9 out of the 14 zero-shot datasets are used. 4) Zero-shot image-text retrieval on MS-COCO captions. 5) Transfer Learning: to further evaluate the generalization of the learned representations, we fine-tune the pretrained backbone for object detection on MS-COCO with ResNet-50 and Mask R-CNN [46] following DenseCLIP [47]. Main Result. Downstream performance is summarized in Table 2(a) and (b). Impressively, the performance of ProtoCLIP matched CLIP with 4× fewer pretraining epochs, which demonstrates that ProtoCLIP significantly improves the representation learning efficiency. Zero-shot accuracies for each dataset can be found in Appendix C, which shows that ProtoCLIP outperforms CLIP on 9 of 14 datasets. Compared to linear probing, ProtoCLIP has more advantages in K-NN classification. Linear probing measures the linear separability of the image representations, while K-NN measures whether semantically similar samples are clustered correctly. We argue that ProtoCLIP's advantage in K-NN classification is brought by the prototypical contrast and efficient representation grouping. Clustering evaluation in Appendix E further proves this property. The quality of ProtoCLIP image representations is confirmed by transfer learning for object detection: 8 epoch ProtoCLIP matched the result of 32 epoch CLIP. Interestingly, we found that ProtoCLIP yields notable improvement on retrieval, which is a contradiction of the observation on Conceptual Captions pretraining. We leave

the investigation of this phenomenon to future work. Appendix D presents full results of the above evaluations.

# 5 Conclusion

We have shown that in addition to representation alignment, representation grouping is also an important characteristic of contrastive language image pretraining. The InfoNCE objective groups representations together via randomly emerged anchors, which we found unstable and sensitive to the modality gap. We set up stable and efficient representation grouping via prototypical discrimination (ProtoCLIP) and alleviated the modality gap issue by PBT. PBT also enabled us to introduce external teacher for additional supervision. Empirical results proved that all these novel designs bring improvements to downstream performance.

# **A Implementation of ProtoCLIP**

## A.1 Implementation Details

**Model Architectures.** Following CLIP [1], we use the modified ResNet-50 backbone as the image encoder, which has three differences compared to the original ResNet-50 [42]: 1) there are three 3×3 convolutions as "stem" instead of a single 7×7 convolution [48], an average pooling follows the "stem" instead of max pooling; 2) the modified ResNet-50 performs antialiased rect-2 blur pooling [49]; 3) the final global average pooling layer is replaced with a multi-head self attention [1, 25]-based pooling. We unitize Transformer [1, 25] as the text encoder, which consists of 12 layers, 8 attention heads, and a width of 512. The max sequence length is set to 76. For image and text projection heads, we use the same architecture as SwAV [12], which is a 2-layers MLP with ReLU activation, 2048 hidden units and 128 output units. Other hyperparameters are summarized in Table A.3.

**Training Configurations.** ProtoCLIP is implemented on PyTorch-based OpenCLIP [45] codebase. We employ automatic mixed-precision [50] to reduce the training cost. Same as CLIP [1], we use the Adam optimizer [51] with decoupled weight decay regularization [52]. Gradients are clipped with a maximum norm of 1e5 to prevent model collapse. Learnable temperatures ( $\tau_{\text{CLIP}}$ ,  $\tau_{\text{Proto}}$ ) are initialized with 0.07 and clipped by 100 following CLIP [1]. Weight decay is not applied to these temperatures. Warm-up and cosine learning rate scheduler [53] are adopted. Same as XDC [15], we employ early stop to prevent over-fitting. The learning rate of the image encoder is reduced to zero at 16 of 32 epochs, then locked-image tuning [54] is performed for the rest of 16 epochs.

**Prototype Construction.** We adopt Faiss [55] implemented K-Means for clustering. We cluster the 128-dimensional projected representations (i.e.,  $h^I$ ,  $h^T$ ) of 200,000 samples in each episode to K=20,000 clusters and use the resulting cluster centroids as prototypes. K-Means is optimized for 20 iterations, which we found it sufficient for convergence. We use a pretrained RoBERTa<sub>large</sub><sup>2</sup> as the external teacher. We extract RoBERTa<sub>large</sub> representations off-line to speed-up ProtoCLIP training, and reduce the representation dimension from 1024 to 64 by PCA to save memory cost.

Table A.3: ProtoCLIP Hyperparameters

		~			
Section	Hyperparameter	Value			
	Batch size	512			
Episodic Training	Episode size	200,000			
	Warm-up Episodes	40			
Prototype Construction	Number of clusters in K-Means	20,000			
Frototype Construction	K-means Iterations	20			
	Optimizer	Adam			
	Adam $\beta_1, \beta_2, \epsilon$	0.9, 0.999, 1e-8			
Optimization	Learning Rate	5e-4, cosine decay			
	Weight decay	0.5			
	Maximum gradient norm	1e5			
	Image Encoder	ResNet-50/ResNet-101			
	Image Resolution	224×224			
	Text Encoder	Transformer			
	Text vocabulary size	49408			
Model Architectures	Initial and maximum temperature ( $\tau_{\text{CLIP}}$ , $\tau_{\text{Proto}}$ )	0.07, 100			
	Representation dimension $(d_z)$	1024			
	Projected Representation dimension $(d_h)$	128			
	External Teacher	RoBERTa <sub>large</sub>			

#### A.2 Pretraining Dataset

Conceptual Captions [41] is an webly collected high-quality image-text dataset consist of 3,318,333 sample pairs. The dataset was made public<sup>3</sup> by Google in 2018. Unfortunately, the number of accessible images keeps drooping due to expired image links. This issue is raised by several recent works in the field of VLP [27, 31, 45]. In this work, since we can only collect 2,643,718 images, we randomly sample a 2,500,000 subset (75% of full CC3M) from them to train our ProtoCLIP. Considering the dropping accessibility of image links in Conceptual Captions, we call for the use of this dataset size (2.5M) in future benchmarking for better comparability.

YFCC was created by filtering YFCC100M [19] for images which contain natural language descriptions and/or titles in English. We used the "YFCC15M-v1" filtered by OpenAI [1]. We obtained

<sup>&</sup>lt;sup>2</sup>https://pytorch.org/hub/pytorch\_fairseq\_roberta

<sup>3</sup>https://github.com/google-research-datasets/conceptual-captions

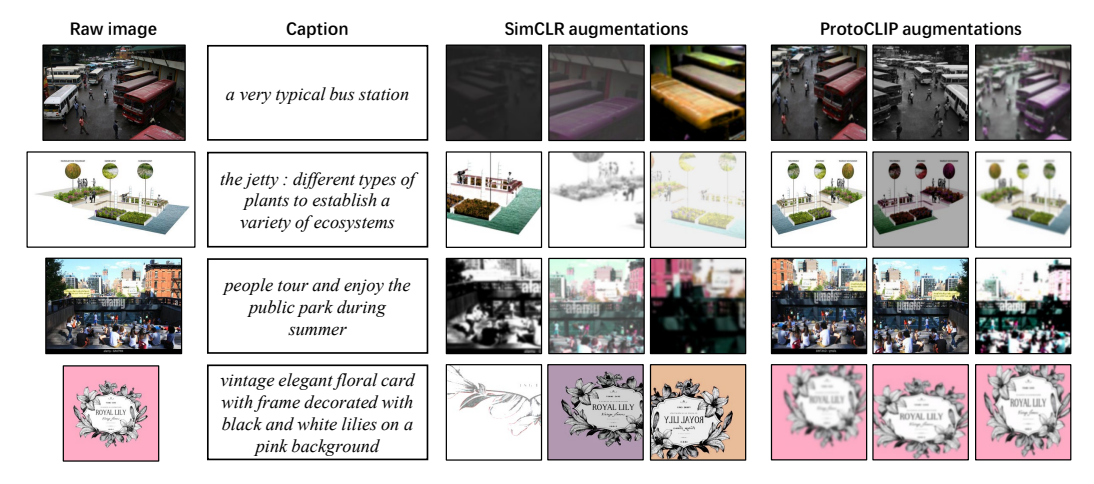


Figure A.5: Visualization of different data augmentations. ProtoCLIP augmentations maintain higher semantic consistency on non-iconic images in Conceptual Captions.

about 14M out of the total 15M samples due to broken links, and used 14,000,000,000 of them to train the ProtoCLIP.

#### A.3 Data Augmentations

Recent advances in VLP [26, 29, 31] have shown that applying random data augmentations can be beneficial. However, we found that common data augmentation strategies used in image SSL is too aggressive in the VLP scenario. As shown in Figure A.5, standard SimCLR [6] augmentations have a higher chance of changing semantics when it is applied to non-iconic images of Conceptual Captions dataset<sup>4</sup>. Such semantic inconsistency poses extra difficulty to image-text representation alignment. To this end, we design a lighter data augmentation to train ProtoCLIP by making two modifications to the SimCLR augmentations parameters: 1) images are randomly resized and cropped with a scale range of 50% to 100% instead of 8% to 100%; 2) probability of applying color jittering is reduced from 0.8 to 0.2. As Figure A.5, such data augmentation maintains higher semantic consistency than that of SimCLR augmentations.

We note that, with applied random data augmentations, our proposed episodic training strategy and PBT can implicitly create additional contrastive supervision for image representations. Recall that episodic training consists of three steps including 1) feature extraction, 2) prototype construction, and 3) model training. Since the first and the third step is performed independently, different augmentations are drawn and applied to the same image. During the model training step, the representation of an image is pushed to the assigned and translated centroid of its another view built in the feature extraction step, leading to an additional contrastive supervision.

Such implicit contrast shares some similarities with SwAV and DeepCluster-v2 that learn visual representations by "contrasting cluster assignments" [12]. However, they use the cluster assignment to set up within-modal supervision, while the implicit contrast of ProtoCLIP is done through the text representation space. Recent SLIP [29] and DeCLIP [31] also applied data augmentation-based contrast to boost VLP performance. However, they contrasted image representations explicitly by forward additional views of images in each training step, which leads to a significantly expanded memory footprint and decreased maximum allowed batch size. In our ProtoCLIP, two views for the implicit contrast are built separately during feature extraction and model training. Although it leads to additional time consumption, the maximum allowed batch size is not affected.

#### A.4 Pseudo Codes

We present PyTorch-style pseudo codes of ProtoCLIP training loop in Algorithm 1 for better understanding of our implementation. For simplicity, here we do not involve the use of external teacher.

<sup>&</sup>lt;sup>4</sup>Several recent works of image SSL have also pointed out that applying SimCLR augmentations on non-iconic scenes images is not optimal. For more details please see ORL [56] and UniVIP [57].

<sup>&</sup>lt;sup>5</sup>Many recent studies have proved that sufficiently large batch size is crucial for contrastive learning [58].

The external teacher supervisions are implemented in the same way of image-text supervisions. Training codes of ProtoCLIP will be made public.

#### **B** Details of ProtoCLIP Evaluation

**Zero-shot Classification.** We use the 1024-dimensional L2-normalized representations (i.e.,  $z^I, z^T$ ) extracted by image and text encoders to perform zero-shot classification. Class names and prompt templates are consistent with CLIP [1] in spite of minor explanations to some classes, e.g., "kite"  $\rightarrow$  "kite (bird of prey)" are added following CLOOB [27]. A total of 14 datasets are adopted: including ImageNet [18], DTD [59], Food101 [60], Oxford-IIIT Pet [61], RenderedSST2 [1], Birdsnap [62], Country211 [1], Flowers102 [63], GTSRB [64], UCF101 [65], Stanford Cars [66], CIFAR10, CIFAR100 and STL10, whose details are summarized in Table A.4. Similar to the Conceptual Captions dataset, the Birdsnap dataset also faces the problem of link expiration. Same as CLIP [1] and CLOOB [27], we use the resources that are available online at the time of writing.

-	1401	C A.T. Datase	et used in zero-snot classification evaluation.
Dataset	Classes	Testset Size	Description
ImageNet	1,000	50,000	1000 categories of objects
DTD	47	1,880	47 categories of texture patches
Food101	101	25,250	101 categories of food dishes
Oxford-IIIT Pet	37	3,669	37 breeds of cats and dogs
RenderedSST2	2	1,821	2 classes of positive or negative movie reviews rendered as text
Birdsnap	500	1,855	500 categories of North American bird species
Country211	211	21,100	211 countries represented by geo-tagged images
Flowers 102	102	6,149	102 species of common UK flowers
GTSRB	43	12,630	43 categories of German traffic signs
UCF101	101	11,213	101 categories of human actions using the middle frame of each clip
Stanford Cars	196	8,041	196 categories of cars (make, model, and year)
CIFAR10	10	10,000	10 categories of animals and vehicles
CIFAR100	100	10,000	100 categories of animals, vehicles, plants, objects, scenes, people
STL10	10	8,000	10 categories of animals and vehicles

Table A.4: Dataset used in zero-shot classification evaluation

**Linear Probing.** Frozen 1024-dimensional image representations ( $z^I$ ) before normalization are used for linear probing. For small-scale CIFAR10, CIFAR100, and STL10, we train a logistic regression classifier using scikit-learn's L-BFGS implementation, with a maximum of 1,000 iterations following CLIP [1]. For larger ImageNet dataset, we adopt PyTorch-based SGD optimization following MoCo [34], SwAV [12] and SLIP [29] to utilize GPU efficiency. Specifically, we train a linear classifier for 100 epochs with a batch size of 256, a learning rate of 0.3, and a weight decay of 1e-6. SGD optimizer with a momentum of 0.9 and cosine learning rate scheduler are applied.

**K-NN Classification.** Following DINO [67], we applied K-NN classification to evaluate the quality of image representations. We build K-NN classifiers based on the training set representations, then measure the top-1 classification accuracy on testing set. K-NN is less sensitive to hyper-parameters compared to linear probing, and we set K=20 for all datasets [67].

**Image-text Retrieval.** Image-text retrieval task consists of image to text retrieval and text to image retrieval. The performance is evaluated on MS-COCO [44] benchmark under the zero-shot setting (i.e., without fine-tuning). The dot-similarity of L2-normalized 1024-dimensional image and text representations  $(z^I, z^T)$  are used for ranking. We report recall@1, recall@5 and recall@10 and their average as mean recall.

**Object Detection.** The image encoder is transferred to perform object detection. We adopted Mask R-CNN detector [46], and fine-tune the pretrained encoder on MS-COCO dataset for 12 epochs following DenseCLIP [47].

# C Full Results of Conceptual Captions Pretraining

Full results of ProtoCLIP hyper-parameter tuning (Section 4.1) are shown in Table A.5. The best values that adopted in ProtoCLIP benchmarking is marked in blue. Performance drop of using other values compared to the best values are also noted. Table A.6 presents full results of zero-shot

evaluation in Table 1 in Section 4.2. Chance performance is reported in the last row as "Random". Table A.7 presents retrieval performance in Table 1.

Table A.5: Full ProtoCLIP hyper-parameter ablation results on Conceptual Captions 1M data (20 epoch).

The results correspond to the Figure 4 in main text.

Episode Size	C10	C100	STL10	Avg.
10k	64.95	37.58	80.85	61.13 (\psi 7.64)
50k	69.19	40.82	86.73	65.58 (\ 3.19)
0.1M	73.17	45.43	87.28	68.63 (\ 0.14)
0.2M	72.87	46.43	87.01	68.77
0.3M	71.97	45.46	87.41	$68.28 (\downarrow 0.49)$
0.7M	71.69	43.18	87.44	67.44 (\ 1.33)
1M	70.55	41.94	85.23	65.91 (\ 2.86)

C10	C100	STL10	Avg.
71.46	41.53	87.15	66.71 (\ 1.58)
71.98	42.14	86.66	66.93 (\ 1.36)
71.87	42.52	86.65	67.01 (\( \psi 1.28 )
71.52	43.55	86.90	67.32 (\psi 0.97)
73.39	45.1	86.38	68.29
73.18	44.46	86.85	68.16 (\psi 0.13)
73.11	45.58	85.54	$68.08 (\downarrow 0.21)$
72.64	43.79	85.91	67.45 (\\$\tau 0.84)
	71.46 71.98 71.87 71.52 <b>73.39</b> 73.18 73.11	71.46 41.53 71.98 42.14 71.87 42.52 71.52 43.55 <b>73.39</b> 45.1 73.18 44.46 73.11 <b>45.58</b>	71.46 41.53 87.15 71.98 42.14 86.66 71.87 42.52 86.65 71.52 43.55 <b>86.90</b> <b>73.39</b> 45.1 86.38 73.18 44.46 86.85 73.11 <b>45.58</b> 85.54

(a) Episode size

(b) Target temperature

Images per Prototype	C10	C100	STL10	Avg.
3	71.61	44.22	87.66	67.83 (\ 0.61)
5	72.09	45.31	87.81	68.40 (\psi 0.04)
10	72.52	45.57	87.23	68.44
20	71.74	45.15	87.21	68.03 (\ 0.41)
50	70.33	44.96	86.23	67.17 (\ 1.27)

Method	C10	C100	STL10	Avg.
CLIP	73.22	44.72	85.15	67.70
ProtoCLIP	75.24	47.33	87.21	69.93
ProtoCLIP + CLIP Text	75.93	48.84	85.40	70.06
ProtoCLIP + RoBERTa	76.29	50.14	86.05	<u>70.83</u>

(d) External teacher

Table A.6: **Full zero-shot classification** evaluation results of Conceptual Captions pretraining (Table 1(b)). "Random" indicates the chance performance.

Batch size	Data	Epoch	Method	ImageNet top-1	ImageNet top-5	CIFAR10	CIFAR100	STL10	Bidsnap	Country211	Flowers 102	GTSRB	UCF101	Stanford Cars	10 Dataset Avg.	6 Dataset Avg.
		16	ProtoCLIP	20.39	40.02	52.57	21.08	87.46	1.62	0.60	13.82	3.43	23.61	1.03	22.56	7.35
512	2.5M	32	CLIP	19.46	38.42	51.74	22.85	81.05	2.05	0.69	12.96	6.02	20.86	1.07	21.87	7.27
312	2.5111	32	ProtoCLIP	21.47	40.84	51.93	23.43	84.66	1.88	0.62	13.97	4.57	21.68	0.98	22.52	7.28
		64	CLIP	20.34	39.21	55.60	23.49	82.31	1.94	0.59	13.16	8.23	22.26	1.12	22.90	7.88
512	2.9M	31	CLOOB	23.97	-	-	-	-	3.06	0.67	13.45	6.38	22.26	1.23	-	7.84
312	2.7111	31	CLIP	20.33	-	-	-	-	2.26	0.67	12.56	7.66	20.98	0.91	-	7.51
-	-	-	Random	0.1	0.5	10	1	11.4	0.02	0.5	1.5	5.9	1.3	0.8	3.25	1.67

Table A.7: Full image-text retrieval results on MS-COCO dataset of Conceptual Captions pretraining (Table 1(b)).

		Image to Tex	ĸt				
Method	Recall@1	Recall@5	Recall@10	Recall@1	Recall@5	Recall@10	Mean Recall
16 Epoch ProtoCLIP	20.00	42.60	54.82	15.32	35.90	47.43	36.01
32 Epoch CLIP	20.12	43.96	56.32	15.52	35.60	47.35	36.48
32 Epoch ProtoCLIP	19.68	42.84	54.90	14.95	35.28	46.52	35.69
64 Epcoh CLIP	20.96	45.34	58.16	16.07	36.84	48.31	37.61

# **D** Full Results of YFCC Pretraining

Here we present full results of zero-shot classification (Table A.8), linear probing and K-NN classification (Table A.9), zero-shot image-text retrieval (Table A.10) and MS-COCO object detection (Table A.11). These results are correspond to the Table 2 in the main text.

# **E** Additional Experiments

**Ablation on ProtoCLIP loss function.** Here we study the effectiveness of each loss term in the ProtoCLIP loss function (Eq. 8). Table A.12a summarizes the results of ImageNet linear probing accuracy. Adding  $\mathcal{L}_{Proto}$  to  $\mathcal{L}_{CLIP}$  improves representation grouping and improves linear accuracy by +3.78%, introducing the external teacher further yields +1.79% improvement.

<sup>(</sup>c) Images per prototype

Table A.8: Full zero-shot classification evaluation results of YFCC pretraining (Table 2(a)).

Arch.	Method	Data	Epoch	Birdsnap	CIFAR10	CIFAR100	Country211	DTD	Flowers102	Food101	GTSRB	OxfordIIITPet	RenderedSST2	StanfordCars	STL10	UCF101	ImageNet	14 Dataset Avg
RN50	CLIP	15M	32	21.81	49.12	20.32	6.34	17.55	50.24	42.80	9.57	27.45	49.92	3.99	79.14	24.32	32.72	31.09
	ProtoCLIP	14M	8	19.92 -1.88	53.95 <b>+4.83</b>	24.60 + <b>4.28</b>	7.14 <b>+0.80</b>	20.00 +2.45	50.51 <b>+0.28</b>	38.61 -4.19	7.19 -2.38	23.88 -3.57	50.08 + <b>0.16</b>	4.68 <b>+0.68</b>	86.13 <b>+6.99</b>	27.84 +3.52	32.02 -0.70	31.90 <b>+0.80</b>
RN101	CLIP ProtoCLIP	15M 14M	32 8	22.94 19.49	52.99 57.23	22.94 26.50	6.82 7.92	18.24 19.68	50.40 52.02	44.18 39.60	9.41 7.34	30.25 25.78	49.92 50.03	3.69 5.04	86.68 88.75	27.44 28.26	34.84 33.80	32.91 32.96
				-3.45	+4.24	+3.56	+1.10	+1.44	+1.63	-4.58	-2.07	-4.47	+0.11	+1.34	+2.08	+0.82	-1.04	+0.05

Table A.9: Full linear probing and K-NN classification evaluation results of YFCC pretraining (Table 2(a)).

Arch.	Method	Data	Epoch		R10	CIFA	R100	DI	D	Food	101	Oxford	IIITPet	Renden	edSST2	Stanfo	rdCars	STI	L10	Imag	eNet	9 Datas	et Avg.
Aicii.	Wichiod	Data	Lpoen	Linear	KNN	Linear	KNN	Linear	KNN	Linear	KNN	Linear	KNN	Linear	KNN								
RN50	CLIP	15M	32	83.65	78.31	62.41	54.11	66.60	62.13	72.82	64.02	66.50	43.12	55.96	51.84	28.26	17.52	94.16	93.34	61.54	55.96	65.77	57.82
KNSU	ProtoCLIP	14M	8	82.84	78.07	61.28	53.95		65.69	69.62	60.13	67.10	45.52		51.46	27.67	19.67	94.16	93.28	62.13	56.72	65.45	
				-0.81	-0.24	-1.13	-0.16	+3.14	+3.56	-3.20	-3.89	+0.60	+2.40	-1.48	-0.38	-0.58	+2.15	0.00	-0.06	+0.59	+0.76	-0.32	+0.46
RN101	CLIP	15M	32	83.37	78.89	62.07	53.42	67.50	62.02	74.08	65.85	66.18	46.25	56.95	52.33	27.70	19.14	94.81	95.03	63.10	57.85	66.19	58.98
KINIUI	ProtoCLIP	14M	8	83.34	79.57	60.58	55.76	70.43	66.28	70.00	62.17	66.94	45.13	55.30	49.48	23.78	20.26	95.09	94.70	62.90	58.05	65.37	59.04
				-0.03	+0.68	-1.49	+2.34	+2.93	+4.26	-4.08	-3.68	+0.76	-1.12	-1.65	-2.86	-3.92	+1.12	+0.27	-0.33	-0.20	+0.19	-0.82	+0.07

**Ablation on ProtoCLIP Augmentation.** Table A.12b compares different data augmentation strategies. "No Augmentation" refers to using only the resize and crop with a random scale between 90% and 100%, which achieves the best image-text retrieval performance. Adding SimCLR augmentations degenerates all downstream performance. Our modified augmentations ("ProtoCLIP Augmentation") improve the retrieval performance compared to "SimCLR Augmentation", and achieve the best ImageNet linear classification and zero-shot classification performance.

Clustering Evaluation. Figure A.6 visualizes the learned representations of CLIP and Proto-CLIP via T-SNE [68]. Proto-CLIP groups "cat", "dog", and "monkey" better. It also gives better separation between "airplane" and "ship", "truck" and "car". These observations can be proved by comparing clustering performance. We cluster the representations to 10 classes by K-Menas and compare the obtained pseudo labels with ground truth labels. Representations of Proto-CLIP yields better adjusted rand index  $(0.673 \rightarrow 0.732)$  and adjusted mutual information  $(0.744 \rightarrow 0.788)$ .



Figure A.6: T-SNE visualizations of CLIP (left) and ProtoCLIP (right) representations on STL10. ProtoCLIP yields a more clearly grouped representation space.

Next, we provide full clustering evaluation results of CLIP and ProtoCLIP trained on CC2.5M for 32 epochs. We extract test set image representations and perform K-Means clustering to derive pseudo labels. The number of clusters (K) is determined by the number of ground truth classes. We report the Adjusted Rand Index (ARI) and Adjusted Mutual Information (AMI) in Table A.12c. ProtoCLIP outperforms CLIP in 8 out of 10 datasets.

# F Understanding ProtoCLIP

What and how does ProtoCLIP actually learn? What happens during the episodic training of ProtoCLIP? In this section, we try to answer these questions by visualizing and analyzing the training procedure of ProtoCILP.

**T-SNE Visualizations.** First, we randomly sample an episode with 200,000 samples, construct 20,000 prototypes, and show T-SNE [68] visualizations of untrained and trained ProtoCLIP representations. As in Figure A.7, learned image and text representations are well grouped. Interestingly, we found that random image and text representation spaces look quite different: random image representations are distributed almost uniformly, but random text space already contains some weak grouping information. We call such information in random text representations as the "first pot of gold" for ProtoCLIP training. It is caused by the fact that texts are human-generated signals, that are highly semantic and information-dense [69]. It has higher level of intrinsic semantics compared to image. Therefore, even

Table A.10: Full image-text retrieval results on MS-COCO dataset of YFCC pretraining (Table 2(a)).
--

Arch,	Method	Data	Epoch	I2T R@1	I2T R@5	I2T R@10	T2I R@1	T2I R@5	T2I R@10	Mean Recall
RN50	CLIP ProtoCLIP	15M 14M	32 8	26.46 30.20 + <b>3.74</b>	52.12 55.08 <b>+2.96</b>	63.82 66.54 <b>+2.72</b>	16.47 16.89 <b>+0.42</b>	37.23 37.93 <b>+0.70</b>	49.11 49.40 <b>+0.29</b>	40.87 42.67 <b>+1.81</b>
RN101	CLIP ProtoCLIP	15M 14M	32 8	29.26 31.46 + <b>2.20</b>	55.12 57.78 + <b>2.66</b>	67.16 69.28 + <b>2.12</b>	17.69 18.17 + <b>0.47</b>	39.15 39.87 + <b>0.71</b>	50.57 51.46 + <b>0.89</b>	43.16 44.67 <b>+1.51</b>

Table A.11: Full object detection results on MS-COCO dataset of YFCC pretraining (Table 2(b)).

Model	Pretraining Epochs	$AP^b$	$AP_{50}^{b}$	$AP_{75}^b$	$AP_S^b$	$AP_M^b$	$AP_L^b$	$AP^m$	$AP_{50}^{m}$	$AP_{75}^m$	$AP_S^m$	$AP_{M}^{m}$	$AP_L^m$
CLIP	32	36.5	58	39.4	21.9	39.4	47.1	34.2	55.1	36.3	16.7	36.7	49.4
ProtoCLIP	8	36.4	58.1	39.3	22.2	39.4	47.6	34.4	55.3	36.7	17.2	36.9	49.9

based on low-level text features (e.g., word appearance), random text encoders of ProtoCLIP can discover some basic semantic similarities.

**Prototype Assignment Visualizations.** The "first pot of gold" can be observed from the visualizations of the prototype assignment. In Figure A.10, A.11, A.12, and A.13, we visualize the prototype assignment of the four representations spaces of Figure A.7. Samples are sorted by the distance to the prototype (horizontal axis) and the number of samples in the cluster (vertical axis). The first row correspond to the largest cluster, while the leftmost column contains samples that are closest to their prototype. We only show the clusters that have more than ten samples for better visualization. From Figure A.10 we can see that samples in the large random text clusters contain identical or very similar captions. These clusters yield high-quality semantic supervision to the image encoder at the very beginning of ProtoCLIP training as "first pot of gold" <sup>6</sup>. However, at the bottom of Figure A.10, random text representations struggle to provide semantic consistent clusters beyond identical captions. Comparatively, learned text representations (Figure A.11) yields much better clusters. For image representations, same as observed in previous image SSL works [11, 37], clusters of random image representations (Figure A.12) prefer to construct clusters according to low-level visual features (especially colors). Comparatively, as shown in Figure A.13, the learned image representations of ProtoCLIP discover various high-level concepts, including statues, markets, graduation ceremony, benches, houses, etc.

**Loss Curves.** We further visualize the loss curves of  $\mathcal{L}_{Proto}$  and  $\mathcal{L}_{Proto}^{external}$  in Figure. A.8. The curves of the image to text loss (red) and text to image loss (blue) have similar trends, but their losses *w.r.t.* the external teacher (gray curves) are quite different: text to external loss is much lower than that of image. This can also be reflected by the pseudo label classification accuracy. Initial random text representation achieves a 6% accuracy for the pseudo label of external teacher and reaches 24% by

<sup>&</sup>lt;sup>6</sup>We note that Florence [70] also used samples with identical captions to benefit VLP models. However, Florence requires constructing an additional hash-table to find samples with identical captions, while ProtoCLIP can discover such samples automatically via clustering.

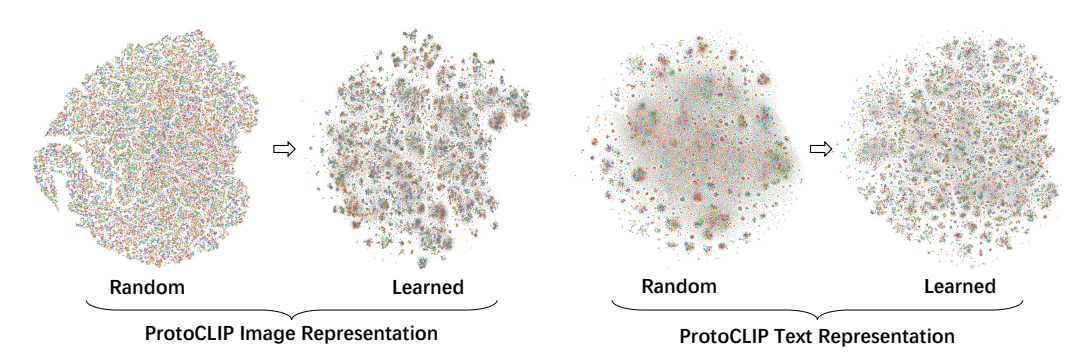


Figure A.7: T-SNE visualizations of ProtoCLIP representations on an episode with 200,000 samples. Colors indicate prototype assignment (Color assignment looks chaotic since there are a total of 20,000 prototypes but only 10 different colors).

Table A.12: Additional experiment results. (a): ablation study of ProtoCLIP loss function (CC2.5M, 8 epochs); (b): ablation study of data augmentations (CC2.5M, 8 epochs); (c): clustering evaluation (CC2.5M, 32 epochs).

Loss Terms	ImageNet Linear Probing Accuracy
$\mathcal{L}_{ ext{CLIP}}$	40.98
$\mathcal{L}_{ ext{Proto}}$	36.89
$\mathcal{L}_{ ext{Proto}} + \mathcal{L}_{ ext{CLIP}}$	44.76
$\mathcal{L}_{ ext{Proto}} + \mathcal{L}_{ ext{CLIP}} + \mathcal{L}_{ ext{Proto}}^{ ext{ external}}$	46.55

Data Augmentation	ImageNet Linear Acc.	ImageNet Zero-shot	Mean Recall
No Augmentation	44.39	11.17	24.45
SimCLR Augmentation ProtoCLIP Augmentation	43.60 <b>46.55</b>	10.05 <b>11.96</b>	20.28
FIOLOCLIF Augmentation	40.55	11.50	21.03

(a) Ablation study of ProtoCLIP loss function

|--|

	Imag	geNet	CIFA	R 10	CIFA	R100	STI	L10	Bids	snap	Count	ry211	Flowe	ers102	GT	SRB	UCI	7101	Stanfo	rd Cars	10 Dat	aset Avg.
	ARI	AMI	ARI	AMI	ARI	AMI	ARI	AMI	ARI	AMI												
CLIP	0.128	0.343	0.270	0.401	0.130	0.340	0.673	0.744	0.033	0.060	0.016	0.091	0.427	0.651	0.169	0.450	0.305	0.579	0.020	0.103	0.216	0.373
ProtoCLIP																	0.360				0.233	

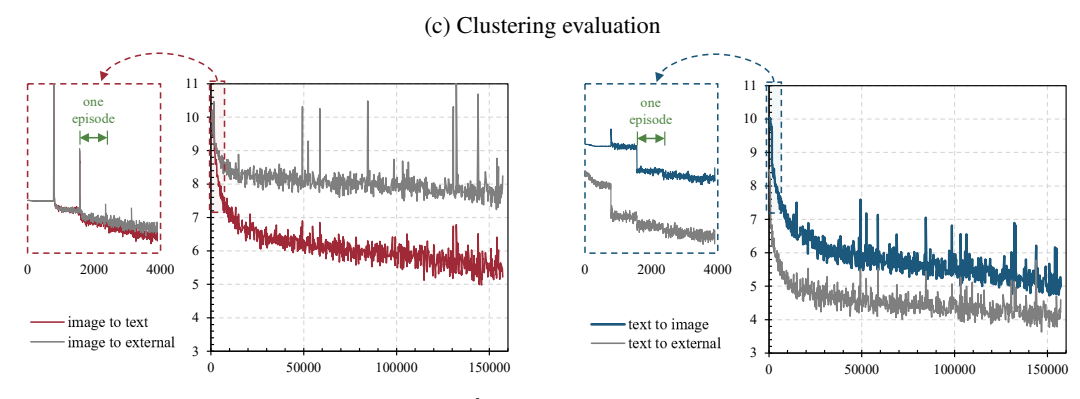


Figure A.8: Loss curves of  $\mathcal{L}_{Proto}$  and  $\mathcal{L}_{Proto}^{external}$ . Text to external loss is lower and converges faster, probably due to the "first pot of gold" effect and the fact that the RoBERTa external teacher is more "friendly" to the text encoder. Zoom-in of the first five episodes shows that frequent prototype update is beneficial.

the end of training. Comparatively, random image representation has zero accuracy and reaches only 5% by the end. We argue that the initial 6% accuracy of text to external teacher reflects the "first pot of gold" of ProtoCLIP training, while the reason for text achieving lower loss and higher accuracy than that of the image is probably that the RoBERTa external teacher is more "friendly" to the text encoder. In addition, we also zoom in on the loss curve of the first five episodes in Figure. A.8 and confirm that frequent prototype update benefits ProtoCLIP convergence.

Efficiency Analysis of Episodic Training. We analyze the time consumption of each step in the episodic training. On a  $8\times2080\text{Ti}$  machine with 60 CPUs and 300G RAM, one episode takes an average of 6 minutes. As shown in Figure A.9, episodic training of ProtoCLIP requires an additional feature extraction step compared to CLIP, which takes 31.0% time. *K*-Means clustering takes only 2.3% of time, since the number of samples in an episode is not too large. Smaller episodes also save the total *K*-Means time cost since its time complexity grows superlinearly  $O(m^{d_h \times K+1})$  along the number of samples m to be clustered. The PBT step takes negligible time<sup>7</sup>.



Figure A.9: Time profiling of the episodic training strategy.

# **G** Broader Impacts

In this paper, we present a more effective approach for

Vision Language Pretraining (VLP). We do not foresee major ethical issues associated with this work. However, like other learning algorithms, VLP models should be applied with caution when deployed in real-world scenarios. It is susceptible to biased learning if the algorithm is given with biased data:

<sup>&</sup>lt;sup>7</sup>We improved our implementation of PBT and significantly reduced its time consumption. We move line 65 in Algorithm 1 out of the for loop. This reduce the time complexity of PBT from  $O(M \times K)$  to O(M + K).

the model will learn the inherent properties and structure of the training data, and exhibit biases intrinsically present in the data.

## Algorithm 1 Pseudocode of ProtoCLIP Training (w/o external teacher)

```
# f_I, f_T: ProtoCLIP image and text encoder
               # g_I, g_T: ProtoCLIP image and text projection head
               # dz, dh = 1024, 128: encoder and projection head representation dimension
               # t_CLIP, t_Proto: learnable temperatures
               # t_target = 0.01: target_temperature
              # K = 20,000 (number of clusters for K-Means)
               # episode_size = 200,000
               # dataset_size = 2,500,000 (CC2.5M)
               # total_epochs = 32
11
12
              # image_features, text_features: feature cache (episode_size, dz)
13
              dataset = EpisodicDataset()
14
              total_episodes = int(dataset_size * total_epochs / episode_size)
15
16
17
              for episode in total_episodes:
18
                     # Random episode sampling
                     dataset.episode_index_mapping = np.random.choice(dataset_size, episode_size)
19
20
21
               # --- Episodic Training Step 1: Feature Extraction --- #
22
                     for image, text in dataloader: # load a minibatch with N samples
23
                            with torch.no_grad():
                                   # forward propagation
h_I, h_T = f_I(image), f_T(text) # (N, dh)
24
25
                                   z_{-1}, z_{-1} = z_{-1}(z_{-1}), z_{
26
27
28
                                   image_features.update(z_I)
29
                                   text_features.update(z_T)
30
31
              # --- Episodic Training Step 2: Prototype Construction --- #
                     # K-Means clustering
32
33
                     C_I = KMeans(image_features, K) # (K, dh)
34
                     C_T = KMeans(text_features, K) # (K, dh)
                    # assign pseudo label
label_I = C_I @ image_features.T.argmax(dim=0) # (episode_size,)
label_I = C_I @ text_features.T.argmax(dim=0) # (episode_size,)
# translate cross-modal prototypes to within-modal centorids
C_PBT2T = PBT(text_features, C_I, label_I) # (K, dh)
C_PBT2I = PBT(image_features, C_T, label_T) # (K, dh)
35
36
37
38
39
40
41
              # --- Episodic Training Step 3: Model Training --- #
for image, text in dataloader: # load a minibatch with N samples
42
43
44
                            # forward propagation
45
                            h_I, h_T = f_I(image), f_T(text) # (N, dh)
                            z_I, z_T = g_I(h_I), g_T(h_T) # (N, dz)
46
                           2_1, 2_1 = g_1(n_1), g_1(n_1), # (N, d2)
# compute losses
loss_CLIP = 0.5 * (InfoNCE(h_I, h_T, t_CLIP) + InfoNCE(h_T, h_I, t_CLIP)) # Eq. 1
loss_Proto = 0.5 * (loss_Proto(h_I, C_PBT2I, label_T, t_Proto) + loss_Proto(h_T, C_PBT2T, label_I, t_Proto)) # Eq. 4
47
48
49
                            loss = loss_CLIP + loss_Proto # Eq. 6
51
                            # backward propagation
52
                            loss.backward()
53
                            update(f_I, f_T, g_I, g_T, t_CLIP, t_Proto) # update model parameters
54
55
56
               def loss_Proto(features, target_centroids, label, t_Proto):
57
                     student_scores = features @ target_centroids.T / t_Proto # Eq.3
58
                     target_scores = target_centroids[label] @ target_centroids.T / t_target # Eq.5
59
                     return cross_entropy(student_scores, target_scores.softmax(dim=1))
60
61
               def PBT(features, C, label):
62
63
                     translated_centorids = torch.zeros(K, dz)
64
                     for k in range(K):
                            assigned_samples = torch.where(teacher_labels==k)
65
                            translated_centorids[k] = torch.mean(features[assigned_samples], dim=0)
66
67
                     return translated centorids
68
69
              class EpisodicDataset():
70
                     def __get_item__(episode_index):
    dataset_index = self.episode_index_mapping[episode_index]
71
72
73
                             image, text = self.images[dataset_index], self.texts[dataset_index]
74
                            image = random_augmentation(image)
                            return image, text
75
76
                     def __len__():
                            return episode_size
```

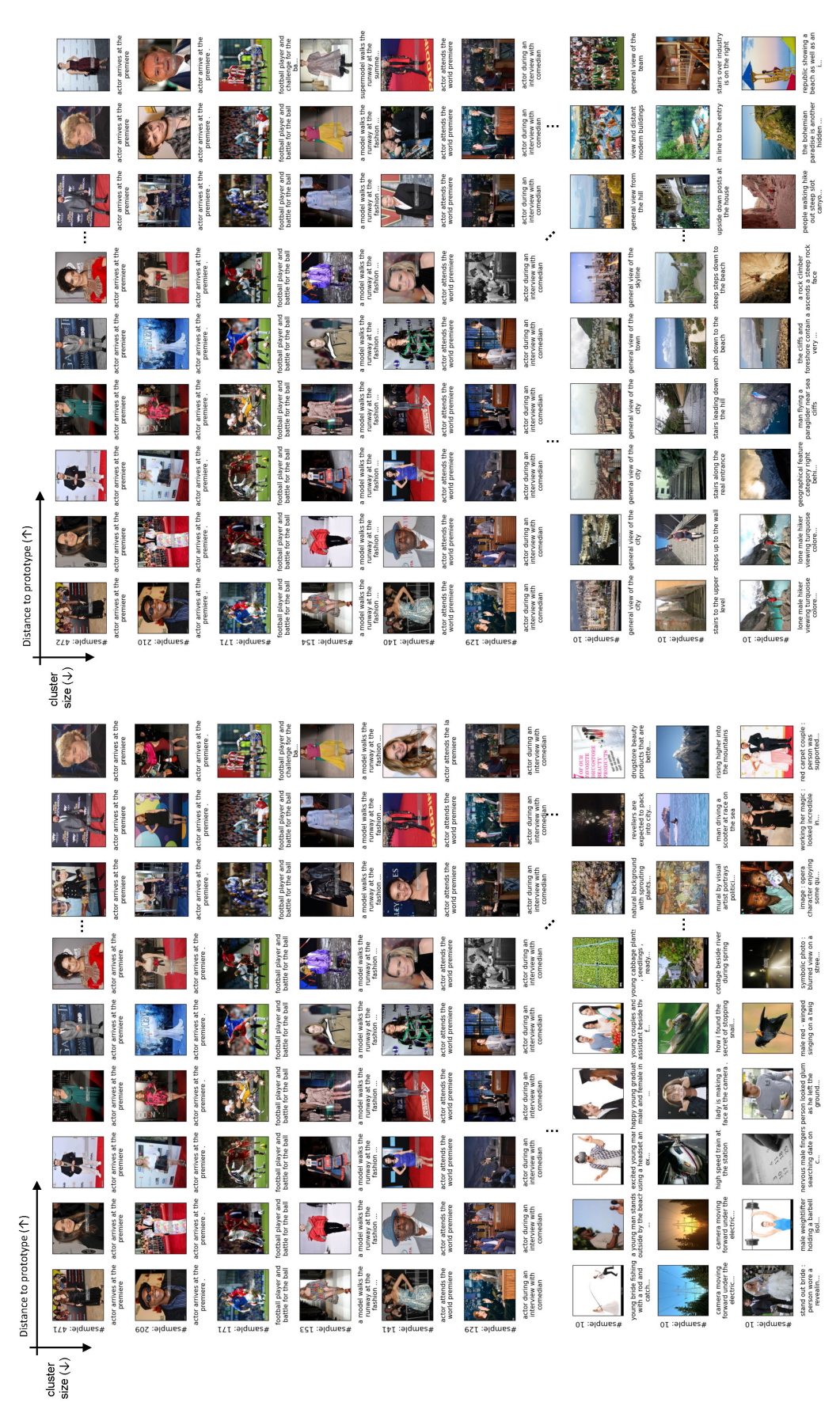


Figure A.10: Prototype assignment of randomly initialized text representations.

Figure A.11: Prototype assignment of trained ProtoCLIP text representations.

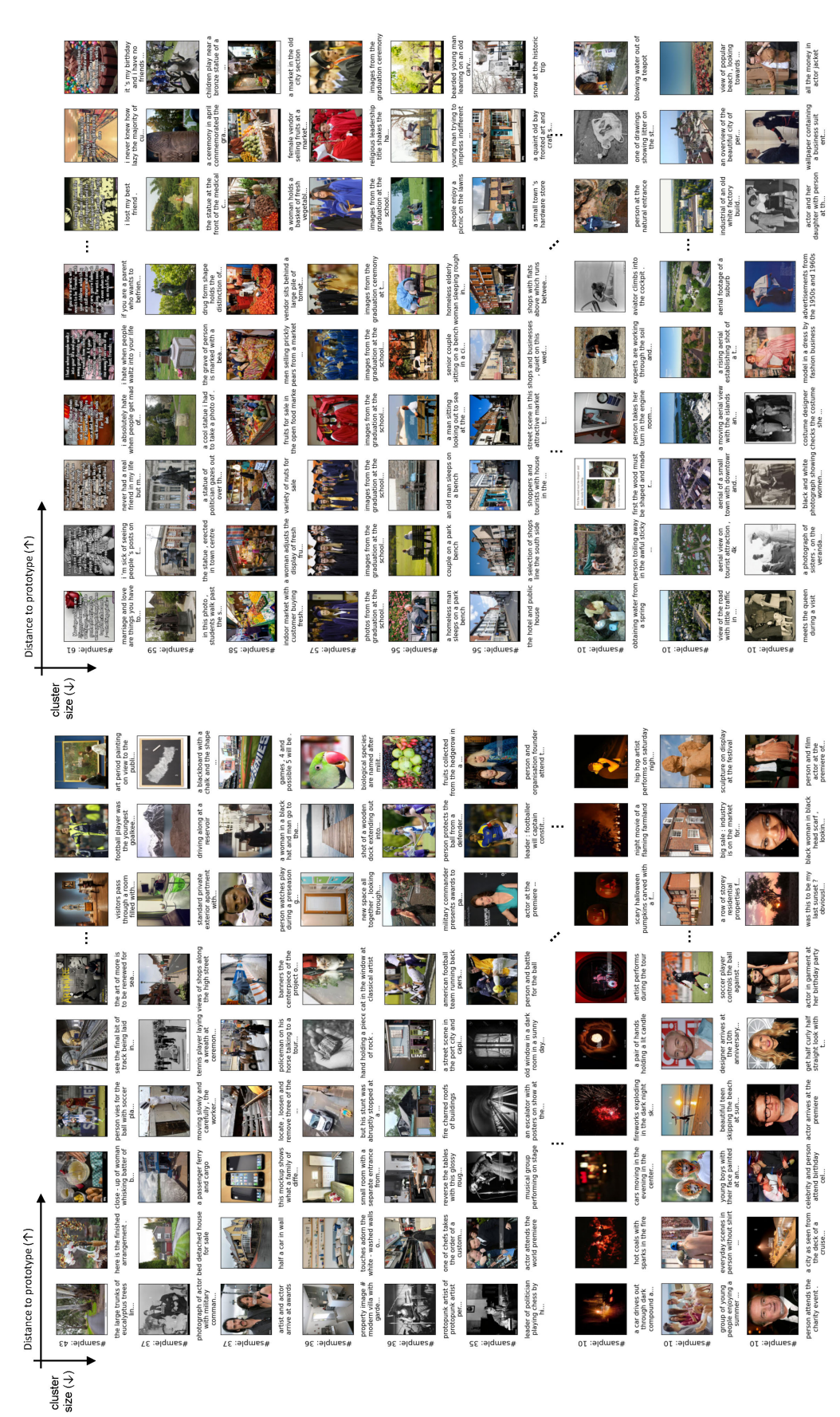


Figure A.12: Prototype assignment of randomly initialized image representations.

Figure A.13: Prototype assignment of trained ProtoCLIP image representations.

## References

- [1] Alec Radford, Jong Wook Kim, Chris Hallacy, Aditya Ramesh, Gabriel Goh, Sandhini Agarwal, Girish Sastry, Amanda Askell, Pamela Mishkin, Jack Clark, Gretchen Krueger, and Ilya Sutskever. Learning transferable visual models from natural language supervision. In Marina Meila and Tong Zhang, editors, *Proceedings of the 38th International Conference on Machine Learning, ICML 2021, 18-24 July 2021, Virtual Event*, volume 139 of *Proceedings of Machine Learning Research*, pages 8748–8763. PMLR, 2021.
- [2] Chao Jia, Yinfei Yang, Ye Xia, Yi-Ting Chen, Zarana Parekh, Hieu Pham, Quoc V. Le, Yun-Hsuan Sung, Zhen Li, and Tom Duerig. Scaling up visual and vision-language representation learning with noisy text supervision. In Marina Meila and Tong Zhang, editors, *Proceedings of the 38th International Conference on Machine Learning, ICML 2021, 18-24 July 2021, Virtual Event*, volume 139 of *Proceedings of Machine Learning Research*, pages 4904–4916. PMLR, 2021.
- [3] Aäron van den Oord, Yazhe Li, and Oriol Vinyals. Representation learning with contrastive predictive coding. *CoRR*, abs/1807.03748, 2018.
- [4] Tongzhou Wang and Phillip Isola. Understanding contrastive representation learning through alignment and uniformity on the hypersphere. In *Proceedings of the 37th International Conference on Machine Learning, ICML 2020, 13-18 July 2020, Virtual Event*, volume 119 of *Proceedings of Machine Learning Research*, pages 9929–9939. PMLR, 2020.
- [5] Yifei Wang, Qi Zhang, Yisen Wang, Jiansheng Yang, and Zhouchen Lin. Chaos is a ladder: A new theoretical understanding of contrastive learning via augmentation overlap. *CoRR*, abs/2203.13457, 2022.
- [6] Ting Chen, Simon Kornblith, Mohammad Norouzi, and Geoffrey E. Hinton. A simple framework for contrastive learning of visual representations. In *Proceedings of the 37th International Conference on Machine Learning, ICML 2020, 13-18 July 2020, Virtual Event*, volume 119 of *Proceedings of Machine Learning Research*, pages 1597–1607. PMLR, 2020.
- [7] Weixin Liang, Yuhui Zhang, Yongchan Kwon, Serena Yeung, and James Zou. Mind the gap: Understanding the modality gap in multi-modal contrastive representation learning. *CoRR*, abs/2203.02053, 2022.
- [8] Geoffrey E. Hinton, Oriol Vinyals, and Jeffrey Dean. Distilling the knowledge in a neural network. CoRR, abs/1503.02531, 2015.
- [9] Lu Yu, Vacit Oguz Yazici, Xialei Liu, Joost van de Weijer, Yongmei Cheng, and Arnau Ramisa. Learning metrics from teachers: Compact networks for image embedding. In *IEEE Conference on Computer Vision and Pattern Recognition*, CVPR 2019, Long Beach, CA, USA, June 16-20, 2019, pages 2907–2916. Computer Vision Foundation / IEEE, 2019.
- [10] Yinhan Liu, Myle Ott, Naman Goyal, Jingfei Du, Mandar Joshi, Danqi Chen, Omer Levy, Mike Lewis, Luke Zettlemoyer, and Veselin Stoyanov. Roberta: A robustly optimized BERT pretraining approach. CoRR, abs/1907.11692, 2019.
- [11] Mathilde Caron, Piotr Bojanowski, Armand Joulin, and Matthijs Douze. Deep clustering for unsupervised learning of visual features. In Vittorio Ferrari, Martial Hebert, Cristian Sminchisescu, and Yair Weiss, editors, Computer Vision ECCV 2018 15th European Conference, Munich, Germany, September 8-14, 2018, Proceedings, Part XIV, volume 11218 of Lecture Notes in Computer Science, pages 139–156. Springer, 2018.
- [12] Mathilde Caron, Ishan Misra, Julien Mairal, Priya Goyal, Piotr Bojanowski, and Armand Joulin. Unsupervised learning of visual features by contrasting cluster assignments. In Hugo Larochelle, Marc' Aurelio Ranzato, Raia Hadsell, Maria-Florina Balcan, and Hsuan-Tien Lin, editors, Advances in Neural Information Processing Systems 33: Annual Conference on Neural Information Processing Systems 2020, NeurIPS 2020, December 6-12, 2020, virtual, 2020.
- [13] Yuki Markus Asano, Christian Rupprecht, and Andrea Vedaldi. Self-labelling via simultaneous clustering and representation learning. In 8th International Conference on Learning Representations, ICLR 2020, Addis Ababa, Ethiopia, April 26-30, 2020. OpenReview.net, 2020.
- [14] Junnan Li, Pan Zhou, Caiming Xiong, and Steven C. H. Hoi. Prototypical contrastive learning of unsupervised representations. In 9th International Conference on Learning Representations, ICLR 2021, Virtual Event, Austria, May 3-7, 2021. OpenReview.net, 2021.
- [15] Humam Alwassel, Dhruv Mahajan, Bruno Korbar, Lorenzo Torresani, Bernard Ghanem, and Du Tran. Self-supervised learning by cross-modal audio-video clustering. In Hugo Larochelle, Marc'Aurelio Ranzato, Raia Hadsell, Maria-Florina Balcan, and Hsuan-Tien Lin, editors, Advances in Neural Information Processing Systems 33: Annual Conference on Neural Information Processing Systems 2020, NeurIPS 2020, December 6-12, 2020, virtual, 2020.

- [16] Yuki Markus Asano, Mandela Patrick, Christian Rupprecht, and Andrea Vedaldi. Labelling unlabelled videos from scratch with multi-modal self-supervision. In Hugo Larochelle, Marc' Aurelio Ranzato, Raia Hadsell, Maria-Florina Balcan, and Hsuan-Tien Lin, editors, Advances in Neural Information Processing Systems 33: Annual Conference on Neural Information Processing Systems 2020, NeurIPS 2020, December 6-12, 2020, virtual, 2020.
- [17] Brian Chen, Andrew Rouditchenko, Kevin Duarte, Hilde Kuehne, Samuel Thomas, Angie W. Boggust, Rameswar Panda, Brian Kingsbury, Rogério Feris, David Harwath, James R. Glass, Michael Picheny, and Shih-Fu Chang. Multimodal clustering networks for self-supervised learning from unlabeled videos. In 2021 IEEE/CVF International Conference on Computer Vision, ICCV 2021, Montreal, QC, Canada, October 10-17, 2021, pages 7992–8001. IEEE, 2021.
- [18] Jia Deng, Wei Dong, Richard Socher, Li-Jia Li, Kai Li, and Li Fei-Fei. Imagenet: A large-scale hierarchical image database. In 2009 IEEE Computer Society Conference on Computer Vision and Pattern Recognition (CVPR 2009), 20-25 June 2009, Miami, Florida, USA, pages 248–255. IEEE Computer Society, 2009.
- [19] Bart Thomee, David A. Shamma, Gerald Friedland, Benjamin Elizalde, Karl Ni, Douglas Poland, Damian Borth, and Li-Jia Li. YFCC100M: the new data in multimedia research. *Commun. ACM*, 59(2):64–73, 2016.
- [20] Dejiao Zhang, Feng Nan, Xiaokai Wei, Shang-Wen Li, Henghui Zhu, Kathleen R. McKeown, Ramesh Nallapati, Andrew O. Arnold, and Bing Xiang. Supporting clustering with contrastive learning. In Kristina Toutanova, Anna Rumshisky, Luke Zettlemoyer, Dilek Hakkani-Tür, Iz Beltagy, Steven Bethard, Ryan Cotterell, Tanmoy Chakraborty, and Yichao Zhou, editors, Proceedings of the 2021 Conference of the North American Chapter of the Association for Computational Linguistics: Human Language Technologies, NAACL-HLT 2021, Online, June 6-11, 2021, pages 5419–5430. Association for Computational Linguistics, 2021.
- [21] Liunian Harold Li, Mark Yatskar, Da Yin, Cho-Jui Hsieh, and Kai-Wei Chang. Visualbert: A simple and performant baseline for vision and language. CoRR, abs/1908.03557, 2019.
- [22] Jiasen Lu, Dhruv Batra, Devi Parikh, and Stefan Lee. Vilbert: Pretraining task-agnostic visiolinguistic representations for vision-and-language tasks. In Hanna M. Wallach, Hugo Larochelle, Alina Beygelzimer, Florence d'Alché-Buc, Emily B. Fox, and Roman Garnett, editors, Advances in Neural Information Processing Systems 32: Annual Conference on Neural Information Processing Systems 2019, NeurIPS 2019, December 8-14, 2019, Vancouver, BC, Canada, pages 13–23, 2019.
- [23] Yen-Chun Chen, Linjie Li, Licheng Yu, Ahmed El Kholy, Faisal Ahmed, Zhe Gan, Yu Cheng, and Jingjing Liu. UNITER: universal image-text representation learning. In Andrea Vedaldi, Horst Bischof, Thomas Brox, and Jan-Michael Frahm, editors, Computer Vision ECCV 2020 16th European Conference, Glasgow, UK, August 23-28, 2020, Proceedings, Part XXX, volume 12375 of Lecture Notes in Computer Science, pages 104–120. Springer, 2020.
- [24] Xiujun Li, Xi Yin, Chunyuan Li, Pengchuan Zhang, Xiaowei Hu, Lei Zhang, Lijuan Wang, Houdong Hu, Li Dong, Furu Wei, Yejin Choi, and Jianfeng Gao. Oscar: Object-semantics aligned pre-training for vision-language tasks. In Andrea Vedaldi, Horst Bischof, Thomas Brox, and Jan-Michael Frahm, editors, Computer Vision ECCV 2020 16th European Conference, Glasgow, UK, August 23-28, 2020, Proceedings, Part XXX, volume 12375 of Lecture Notes in Computer Science, pages 121–137. Springer, 2020.
- [25] Ashish Vaswani, Noam Shazeer, Niki Parmar, Jakob Uszkoreit, Llion Jones, Aidan N. Gomez, Lukasz Kaiser, and Illia Polosukhin. Attention is all you need. In Isabelle Guyon, Ulrike von Luxburg, Samy Bengio, Hanna M. Wallach, Rob Fergus, S. V. N. Vishwanathan, and Roman Garnett, editors, Advances in Neural Information Processing Systems 30: Annual Conference on Neural Information Processing Systems 2017, December 4-9, 2017, Long Beach, CA, USA, pages 5998–6008, 2017.
- [26] Lewei Yao, Runhui Huang, Lu Hou, Guansong Lu, Minzhe Niu, Hang Xu, Xiaodan Liang, Zhenguo Li, Xin Jiang, and Chunjing Xu. FILIP: fine-grained interactive language-image pre-training. CoRR, abs/2111.07783, 2021.
- [27] Andreas Fürst, Elisabeth Rumetshofer, Viet Tran, Hubert Ramsauer, Fei Tang, Johannes Lehner, David P. Kreil, Michael Kopp, Günter Klambauer, Angela Bitto-Nemling, and Sepp Hochreiter. CLOOB: modern hopfield networks with infoloob outperform CLIP. CoRR, abs/2110.11316, 2021.
- [28] Jue Wang, Haofan Wang, Jincan Deng, Weijia Wu, and Debing Zhang. Efficientclip: Efficient cross-modal pre-training by ensemble confident learning and language modeling. *CoRR*, abs/2109.04699, 2021.

- [29] Norman Mu, Alexander Kirillov, David A. Wagner, and Saining Xie. SLIP: self-supervision meets language-image pre-training. *CoRR*, abs/2112.12750, 2021.
- [30] Jacob Devlin, Ming-Wei Chang, Kenton Lee, and Kristina Toutanova. BERT: pre-training of deep bidirectional transformers for language understanding. In Jill Burstein, Christy Doran, and Thamar Solorio, editors, Proceedings of the 2019 Conference of the North American Chapter of the Association for Computational Linguistics: Human Language Technologies, NAACL-HLT 2019, Minneapolis, MN, USA, June 2-7, 2019, Volume 1 (Long and Short Papers), pages 4171–4186. Association for Computational Linguistics, 2019.
- [31] Yangguang Li, Feng Liang, Lichen Zhao, Yufeng Cui, Wanli Ouyang, Jing Shao, Fengwei Yu, and Junjie Yan. Supervision exists everywhere: A data efficient contrastive language-image pre-training paradigm. *CoRR*, abs/2110.05208, 2021.
- [32] Linus Ericsson, Henry Gouk, Chen Change Loy, and Timothy M. Hospedales. Self-supervised representation learning: Introduction, advances and challenges. *CoRR*, abs/2110.09327, 2021.
- [33] Longlong Jing and Yingli Tian. Self-supervised visual feature learning with deep neural networks: A survey. IEEE Trans. Pattern Anal. Mach. Intell., 43(11):4037–4058, 2021.
- [34] Kaiming He, Haoqi Fan, Yuxin Wu, Saining Xie, and Ross B. Girshick. Momentum contrast for unsupervised visual representation learning. In 2020 IEEE/CVF Conference on Computer Vision and Pattern Recognition, CVPR 2020, Seattle, WA, USA, June 13-19, 2020, pages 9726–9735. Computer Vision Foundation / IEEE, 2020.
- [35] Jean-Bastien Grill, Florian Strub, Florent Altché, Corentin Tallec, Pierre H. Richemond, Elena Buchatskaya, Carl Doersch, Bernardo Ávila Pires, Zhaohan Guo, Mohammad Gheshlaghi Azar, Bilal Piot, Koray Kavukcuoglu, Rémi Munos, and Michal Valko. Bootstrap your own latent - A new approach to selfsupervised learning. In Hugo Larochelle, Marc' Aurelio Ranzato, Raia Hadsell, Maria-Florina Balcan, and Hsuan-Tien Lin, editors, Advances in Neural Information Processing Systems 33: Annual Conference on Neural Information Processing Systems 2020, NeurIPS 2020, December 6-12, 2020, virtual, 2020.
- [36] Xinlei Chen and Kaiming He. Exploring simple siamese representation learning. In *IEEE Conference on Computer Vision and Pattern Recognition*, CVPR 2021, virtual, June 19-25, 2021, pages 15750–15758. Computer Vision Foundation / IEEE, 2021.
- [37] Debidatta Dwibedi, Yusuf Aytar, Jonathan Tompson, Pierre Sermanet, and Andrew Zisserman. With a little help from my friends: Nearest-neighbor contrastive learning of visual representations. In 2021 IEEE/CVF International Conference on Computer Vision, ICCV 2021, Montreal, QC, Canada, October 10-17, 2021, pages 9568–9577. IEEE, 2021.
- [38] Mehdi Azabou, Mohammad Gheshlaghi Azar, Ran Liu, Chi-Heng Lin, Erik C. Johnson, Kiran Bhaskaran-Nair, Max Dabagia, Keith B. Hengen, William R. Gray Roncal, Michal Valko, and Eva L. Dyer. Mine your own view: Self-supervised learning through across-sample prediction. *CoRR*, abs/2102.10106, 2021.
- [39] Wonpyo Park, Dongju Kim, Yan Lu, and Minsu Cho. Relational knowledge distillation. In *IEEE Conference on Computer Vision and Pattern Recognition, CVPR 2019, Long Beach, CA, USA, June 16-20, 2019*, pages 3967–3976. Computer Vision Foundation / IEEE, 2019.
- [40] Yufeng Cui, Lichen Zhao, Feng Liang, Yangguang Li, and Jing Shao. Democratizing contrastive languageimage pre-training: A CLIP benchmark of data, model, and supervision. CoRR, abs/2203.05796, 2022.
- [41] Piyush Sharma, Nan Ding, Sebastian Goodman, and Radu Soricut. Conceptual captions: A cleaned, hypernymed, image alt-text dataset for automatic image captioning. In Iryna Gurevych and Yusuke Miyao, editors, Proceedings of the 56th Annual Meeting of the Association for Computational Linguistics, ACL 2018, Melbourne, Australia, July 15-20, 2018, Volume 1: Long Papers, pages 2556–2565. Association for Computational Linguistics, 2018.
- [42] Kaiming He, Xiangyu Zhang, Shaoqing Ren, and Jian Sun. Deep residual learning for image recognition. In 2016 IEEE Conference on Computer Vision and Pattern Recognition, CVPR 2016, Las Vegas, NV, USA, June 27-30, 2016, pages 770–778. IEEE Computer Society, 2016.
- [43] Jianwei Yang, Chunyuan Li, Pengchuan Zhang, Bin Xiao, Ce Liu, Lu Yuan, and Jianfeng Gao. Unified contrastive learning in image-text-label space. *CoRR*, abs/2204.03610, 2022.
- [44] Xinlei Chen, Hao Fang, Tsung-Yi Lin, Ramakrishna Vedantam, Saurabh Gupta, Piotr Dollár, and C. Lawrence Zitnick. Microsoft COCO captions: Data collection and evaluation server. CoRR, abs/1504.00325, 2015.

- [45] Gabriel Ilharco, Mitchell Wortsman, Ross Wightman, Cade Gordon, Nicholas Carlini, Rohan Taori, Achal Dave, Vaishaal Shankar, Hongseok Namkoong, John Miller, Hannaneh Hajishirzi, Ali Farhadi, and Ludwig Schmidt. Openclip, July 2021. If you use this software, please cite it as below.
- [46] Kaiming He, Georgia Gkioxari, Piotr Dollár, and Ross B. Girshick. Mask R-CNN. IEEE Trans. Pattern Anal. Mach. Intell., 42(2):386–397, 2020.
- [47] Yongming Rao, Wenliang Zhao, Guangyi Chen, Yansong Tang, Zheng Zhu, Guan Huang, Jie Zhou, and Jiwen Lu. Denseclip: Language-guided dense prediction with context-aware prompting. CoRR, abs/2112.01518, 2021.
- [48] Tong He, Zhi Zhang, Hang Zhang, Zhongyue Zhang, Junyuan Xie, and Mu Li. Bag of tricks for image classification with convolutional neural networks. In *IEEE Conference on Computer Vision and Pattern Recognition*, CVPR 2019, Long Beach, CA, USA, June 16-20, 2019, pages 558–567. Computer Vision Foundation / IEEE, 2019.
- [49] Richard Zhang. Making convolutional networks shift-invariant again. In Kamalika Chaudhuri and Ruslan Salakhutdinov, editors, Proceedings of the 36th International Conference on Machine Learning, ICML 2019, 9-15 June 2019, Long Beach, California, USA, volume 97 of Proceedings of Machine Learning Research, pages 7324–7334. PMLR, 2019.
- [50] Paulius Micikevicius, Sharan Narang, Jonah Alben, Gregory F. Diamos, Erich Elsen, David García, Boris Ginsburg, Michael Houston, Oleksii Kuchaiev, Ganesh Venkatesh, and Hao Wu. Mixed precision training. In 6th International Conference on Learning Representations, ICLR 2018, Vancouver, BC, Canada, April 30 May 3, 2018, Conference Track Proceedings. OpenReview.net, 2018.
- [51] Diederik P. Kingma and Jimmy Ba. Adam: A method for stochastic optimization. In Yoshua Bengio and Yann LeCun, editors, 3rd International Conference on Learning Representations, ICLR 2015, San Diego, CA, USA, May 7-9, 2015, Conference Track Proceedings, 2015.
- [52] Ilya Loshchilov and Frank Hutter. Decoupled weight decay regularization. In 7th International Conference on Learning Representations, ICLR 2019, New Orleans, LA, USA, May 6-9, 2019. OpenReview.net, 2019.
- [53] Ilya Loshchilov and Frank Hutter. SGDR: stochastic gradient descent with warm restarts. In 5th International Conference on Learning Representations, ICLR 2017, Toulon, France, April 24-26, 2017, Conference Track Proceedings. OpenReview.net, 2017.
- [54] Xiaohua Zhai, Xiao Wang, Basil Mustafa, Andreas Steiner, Daniel Keysers, Alexander Kolesnikov, and Lucas Beyer. Lit: Zero-shot transfer with locked-image text tuning. CoRR, abs/2111.07991, 2021.
- [55] Jeff Johnson, Matthijs Douze, and Hervé Jégou. Billion-scale similarity search with GPUs. *IEEE Transactions on Big Data*, 7(3):535–547, 2019.
- [56] Jiahao Xie, Xiaohang Zhan, Ziwei Liu, Yew Soon Ong, and Chen Change Loy. Unsupervised object-level representation learning from scene images. In Marc'Aurelio Ranzato, Alina Beygelzimer, Yann N. Dauphin, Percy Liang, and Jennifer Wortman Vaughan, editors, Advances in Neural Information Processing Systems 34: Annual Conference on Neural Information Processing Systems 2021, NeurIPS 2021, December 6-14, 2021, virtual, pages 28864–28876, 2021.
- [57] Zhaowen Li, Yousong Zhu, Fan Yang, Wei Li, Chaoyang Zhao, Yingying Chen, Zhiyang Chen, Jiahao Xie, Liwei Wu, Rui Zhao, Ming Tang, and Jinqiao Wang. Univip: A unified framework for self-supervised visual pre-training. *CoRR*, abs/2203.06965, 2022.
- [58] Jordan T. Ash, Surbhi Goel, Akshay Krishnamurthy, and Dipendra Misra. Investigating the role of negatives in contrastive representation learning. In Gustau Camps-Valls, Francisco J. R. Ruiz, and Isabel Valera, editors, International Conference on Artificial Intelligence and Statistics, AISTATS 2022, 28-30 March 2022, Virtual Event, volume 151 of Proceedings of Machine Learning Research, pages 7187–7209. PMLR, 2022.
- [59] Mircea Cimpoi, Subhransu Maji, Iasonas Kokkinos, Sammy Mohamed, and Andrea Vedaldi. Describing textures in the wild. In 2014 IEEE Conference on Computer Vision and Pattern Recognition, CVPR 2014, Columbus, OH, USA, June 23-28, 2014, pages 3606–3613. IEEE Computer Society, 2014.
- [60] Lukas Bossard, Matthieu Guillaumin, and Luc Van Gool. Food-101 mining discriminative components with random forests. In David J. Fleet, Tomás Pajdla, Bernt Schiele, and Tinne Tuytelaars, editors, Computer Vision - ECCV 2014 - 13th European Conference, Zurich, Switzerland, September 6-12, 2014, Proceedings, Part VI, volume 8694 of Lecture Notes in Computer Science, pages 446–461. Springer, 2014.

- [61] Omkar M. Parkhi, Andrea Vedaldi, Andrew Zisserman, and C. V. Jawahar. Cats and dogs. In 2012 IEEE Conference on Computer Vision and Pattern Recognition, Providence, RI, USA, June 16-21, 2012, pages 3498–3505. IEEE Computer Society, 2012.
- [62] Thomas Berg, Jiongxin Liu, Seung Woo Lee, Michelle L. Alexander, David W. Jacobs, and Peter N. Belhumeur. Birdsnap: Large-scale fine-grained visual categorization of birds. In 2014 IEEE Conference on Computer Vision and Pattern Recognition, CVPR 2014, Columbus, OH, USA, June 23-28, 2014, pages 2019–2026. IEEE Computer Society, 2014.
- [63] Maria-Elena Nilsback and Andrew Zisserman. Automated flower classification over a large number of classes. In Sixth Indian Conference on Computer Vision, Graphics & Image Processing, ICVGIP 2008, Bhubaneswar, India, 16-19 December 2008, pages 722–729. IEEE Computer Society, 2008.
- [64] Johannes Stallkamp, Marc Schlipsing, Jan Salmen, and Christian Igel. The german traffic sign recognition benchmark: A multi-class classification competition. In *The 2011 International Joint Conference on Neural Networks, IJCNN 2011, San Jose, California, USA, July 31 - August 5, 2011*, pages 1453–1460. IEEE, 2011.
- [65] Khurram Soomro, Amir Roshan Zamir, and Mubarak Shah. UCF101: A dataset of 101 human actions classes from videos in the wild. CoRR, abs/1212.0402, 2012.
- [66] Jonathan Krause, Michael Stark, Jia Deng, and Li Fei-Fei. 3d object representations for fine-grained categorization. In 2013 IEEE International Conference on Computer Vision Workshops, ICCV Workshops 2013, Sydney, Australia, December 1-8, 2013, pages 554–561. IEEE Computer Society, 2013.
- [67] Mathilde Caron, Hugo Touvron, Ishan Misra, Hervé Jégou, Julien Mairal, Piotr Bojanowski, and Armand Joulin. Emerging properties in self-supervised vision transformers. In 2021 IEEE/CVF International Conference on Computer Vision, ICCV 2021, Montreal, QC, Canada, October 10-17, 2021, pages 9630– 9640. IEEE, 2021.
- [68] Laurens Van der Maaten and Geoffrey Hinton. Visualizing data using t-sne. *Journal of machine learning research*, 9(11), 2008.
- [69] Kaiming He, Xinlei Chen, Saining Xie, Yanghao Li, Piotr Dollár, and Ross B. Girshick. Masked autoencoders are scalable vision learners. CoRR, abs/2111.06377, 2021.
- [70] Lu Yuan, Dongdong Chen, Yi-Ling Chen, Noel Codella, Xiyang Dai, Jianfeng Gao, Houdong Hu, Xuedong Huang, Boxin Li, Chunyuan Li, Ce Liu, Mengchen Liu, Zicheng Liu, Yumao Lu, Yu Shi, Lijuan Wang, Jianfeng Wang, Bin Xiao, Zhen Xiao, Jianwei Yang, Michael Zeng, Luowei Zhou, and Pengchuan Zhang. Florence: A new foundation model for computer vision. *CoRR*, abs/2111.11432, 2021.